nature cell biology

Histone deacetylase and Cullin3–REN^{KCTD11} ubiquitin ligase interplay regulates Hedgehog signalling through Gli acetylation

Gianluca Canettieri[1,6], Lucia Di Marcotullio[1,6], Azzura Greco[1], Sonia Coni[1], Laura Antonucci[1], Paola Infante[1], Laura Pietrosanti[1], Enrico De Smaele[1], Elisabetta Ferretti[1], Evelina Miele[1], Marianna Pelloni[1], Giuseppina De Simone[5], Emilia Maria Pedone[5], Paola Gallinari[3], Alessandra Giorgi[2], Christian Steinkühler[3], Luigi Vitagliano[5], Carlo Pedone[5], M. Eugenia Schininà[2], Isabella Screpanti[1] and Alberto Gulino[1,4,7]

Hedgehog signalling is crucial for development and is deregulated in several tumours, including medulloblastoma. Regulation of the transcriptional activity of Gli (glioma-associated oncogene) proteins, effectors of the Hedgehog pathway, is poorly understood. We show here that Gli1 and Gli2 are acetylated proteins and that their HDAC-mediated deacetylation promotes transcriptional activation and sustains a positive autoregulatory loop through Hedgehog-induced upregulation of HDAC1. This mechanism is turned off by HDAC1 degradation through an E3 ubiquitin ligase complex formed by Cullin3 and REN, a Gli antagonist lost in human medulloblastoma. Whereas high HDAC1 and low REN expression in neural progenitors and medulloblastomas correlates with active Hedgehog signalling, loss of HDAC activity suppresses Hedgehog-dependent growth of neural progenitors and tumour cells. Consistent with this, abrogation of Gli1 acetylation enhances cellular proliferation and transformation. These data identify an integrated HDAC- and ubiquitin-mediated circuitry, where acetylation of Gli proteins functions as an unexpected key transcriptional checkpoint of Hedgehog signalling.

Hedgehog (Hh) is a master regulator of tissue development[1,2]. Under physiological conditions, Hh signalling keeps cerebellar granule cell progenitors (GCPs) proliferating and undifferentiated, whereas its termination allows GCPs to exit the cell cycle and differentiate.

Hh signalling is controlled by extracellular ligands (Shh, Ihh or Dhh) through interaction with the receptor Patched (Ptch), thereby enhancing Smoothened (Smo) function, which activates Gli transcription factors. Transcriptional activation is largely derived from Gli1 and Gli2, whereas Gli3 mainly shows repressor activity in the absence of ligand. Gli1 is a Hh-transcriptional target and a strong constitutive transcriptional activator, which enhances its own expression, thus autoreinforcing the signalling strength[2].

Hh pathway deregulation is responsible for the onset of several tumours, including medulloblastoma (the most frequent childhood brain malignancy), arising from transformed GCPs. Mutations of human and mouse Hh pathway components indicate that withdrawal of Hh activity prevents tumorigenesis. Indeed, persistent uncontrolled Hh signalling leads to GCP overgrowth and eventually transformation[1,2]. In this context, Gli1 functions as an oncogene, as highlighted by its *in vitro* transforming ability[3] and by the reduced medulloblastoma development in *Gli1*$^{-/-}$/*Ptch1*$^{+/-}$ mice[4]. Non-canonical Hh-Gli1 activation, independent of mutations of pathway components or ligand overexpression, is also frequently observed in medulloblastoma and other tumours[2,5]. This emphasizes the importance of the mechanisms that terminate Gli1 activity and that may be impaired in disease. In this regard, although altered ubiquitin-dependent degradation of Gli1 has been documented[6,7], less information is available on the regulation of Gli1 transcriptional activity during development and in cancer cells.

Acetylation represents a key transcriptional event, finely tuned by histone acetyltransferases (HATs) and histone deacetylases (HDACs). HATs activate and HDACs repress transcription by modulating the acetylation status of histones or transcription factors[8]. However, HDAC activity also enhances transcription, depending on the context[9,10]. Although HATs and HDACs are crucial regulators of development and tumorigenesis[8,11], their role in the control of Gli transcriptional activity is poorly understood. Gli3 transcriptional activation requires CREB-binding protein (CBP) and HAT[12], whereas its inhibitory function is mediated by the Ski-dependent recruitment of HDAC, which possibly modulates histone acetylation[13]. In contrast, Gli1 is believed to function through alternative unelucidated mechanisms[12,14].

[1]Department of Experimental Medicine, [2]Department of Biochemical Sciences, Sapienza University, 324 viale Regina Elena, 00161 Rome, Italy. [3]IRBM-Merck Research Laboratories Rome, 00040 Pomezia, Italy. [4]Neuromed Institute, 86077 Pozzilli, Italy. [5]Institute of Biostructures and Bioimaging, CNR, 80134 Napoli, Italy.
[6]These authors contributed equally to this work.
[7]Correspondence should be addressed to A.G. (e-mail: alberto.gulino@uniroma1.it).

Received 21 October 2009; accepted 7 December 2009; published online 17 January 2010; DOI: 10.1038/ncb2013

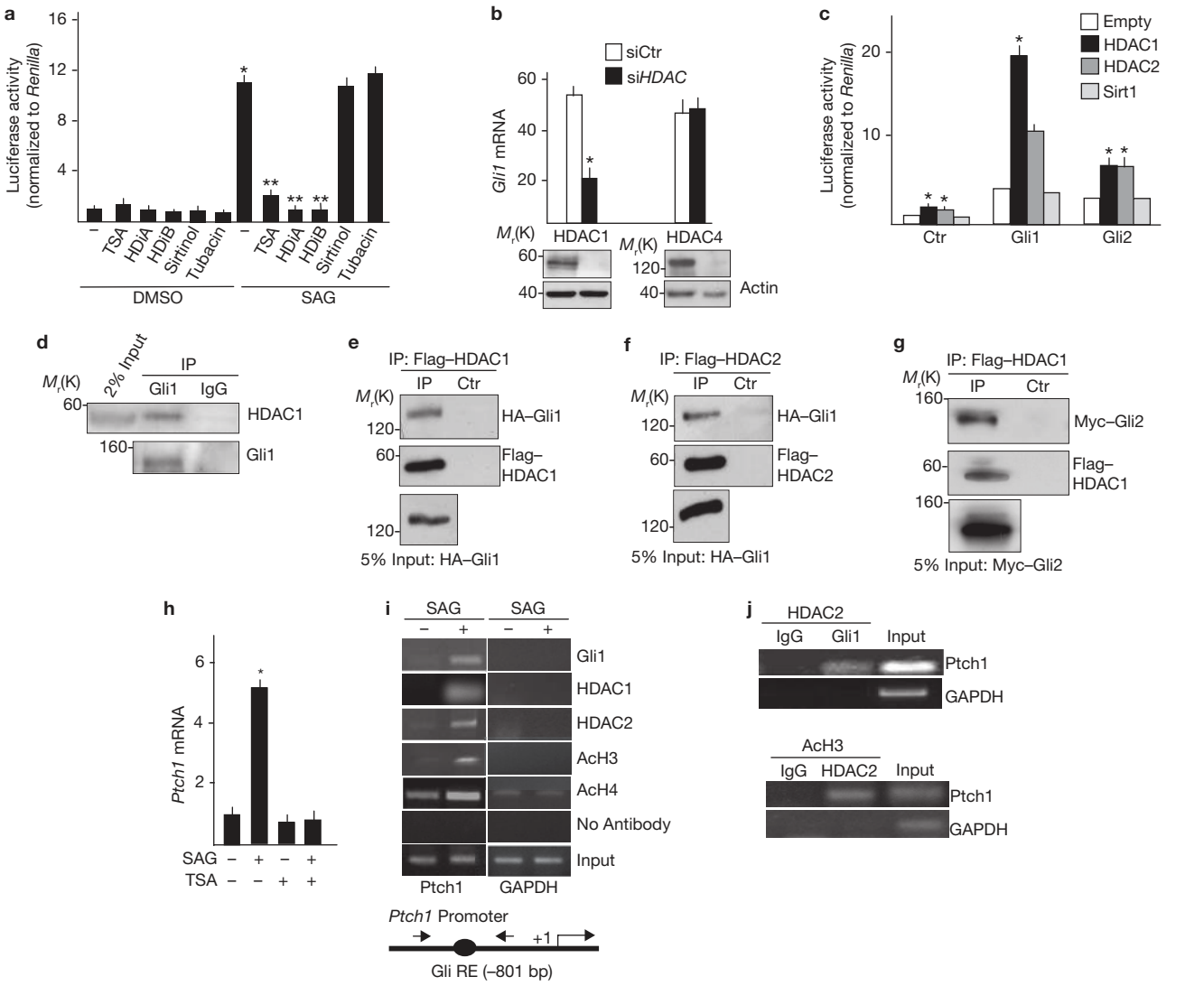

Figure 1 HDAC1 and HDAC2 are transcriptional enhancers of Gli1 activity. (**a**) Shh light II cells were treated for 48 h with SAG or DMSO, and for the last 24 h with HDACi (1 μM TSA, 2 μM HDiA, 2 μM HDiB, 25 μM sirtinol or 2.5 μM tubacin) and luciferase activity tested. $*P < 0.01$, SAG versus control; $**P < 0.01$, SAG + HDACi versus SAG. (**b**) NIH 3T3 cells were transfected with the indicated siRNAs for 72 h and then treated with SAG for 48 h. Levels of mRNA were evaluated by quantitative PCR. $*P < 0.05$. Bottom, levels of HDAC proteins at the end of treatment. (**c**) Luciferase activity in HEK293T cells transfected with 12 × Gli–Luc and PRL-TK *Renilla* (normalization control) plus control, Gli1 or Gli2 vectors alone (Empty) or with HDAC1, HDAC2 or Sirt1. $*P < 0.05$, versus empty. (**d**) Cell lysates from HEK293T cells were immunoprecipitated with Gli1 or control rabbit antisera (IgG) and immunoblotted with anti-Gli1 and anti-HDAC1 antibodies. (**e**–**g**) HEK293T cells co-transfected with Flag–HDACs and HA–Gli1 (**e**, **f**) or Myc–Gli2 (**g**) were immunoprecipitated with anti-Flag agarose beads and immunoblotted with anti-HA, anti-Flag or anti-Myc antibodies. For negative controls, beads were pre-blocked with Flag peptide (0.1 mg ml^{-1}). (**h**) NIH 3T3 cells were treated for 48 h with SAG and/or with TSA for the last 24 h and *Ptch1* mRNA levels were measured by quantitative PCR. $*P < 0.01$, versus control. (**i**) NIH 3T3 cells were treated with SAG for 48 h, and chromatin was immunoprecipitated with the indicated antibodies. Eluted DNA was PCR-amplified using primers encompassing the Gli-binding site (Gli RE) of the *Ptch1* promoter (bottom) or the *GAPDH* coding region (negative control). Data represent composite images of samples from the same blot. (**j**) Chromatin from SAG-treated cells (for 48 h) was immunoprecipitated with anti-HDAC2 (top) or anti-acetyl-H3 (bottom) antibodies and then eluted and immunoprecipitated again with normal rabbit IgG or anti-Gli1 (top), or anti-HDAC2 (bottom) antibodies. Eluted DNA was PCR-amplified with the primers described above. Results in **a**–**c** and **h** are shown as the mean ± s.d. ($n = 3$). Ctr, control. For uncropped images of blots, see Supplementary Information, Fig. S8.

Here, we identify Gli1 and Gli2 acetylation as a key transcriptional checkpoint of Hh signalling, where deacetylation promotes transcriptional activation. We report that Gli deacetylation is regulated by a multiprotein module involving HDAC and an E3 ubiquitin ligase, formed by Cullin3 and REN^{KCTD11}, a Gli antagonist encoded by a gene frequently deleted in human medulloblastoma[15]. Such deacetylation and ubiquitylation mechanisms are involved in Hh-dependent cerebellar GCP and medulloblastoma growth.

RESULTS

Class I HDACs enhance Hh-induced transcriptional activation

To study the role of acetylation in Hh signalling, we tested the effect of HDAC inhibitors (HDACi) on NIH 3T3 Shh light II cells stably incorporating an Hh-responsive reporter[16]. Class I and II HDACi tricostatin A (TSA) and class I HDAC1–2 or HDAC1–3 selective inhibitors (HDiA and HDiB, respectively, Supplementary Information, Fig. S1A) suppressed luciferase activity in cells treated with the Smo

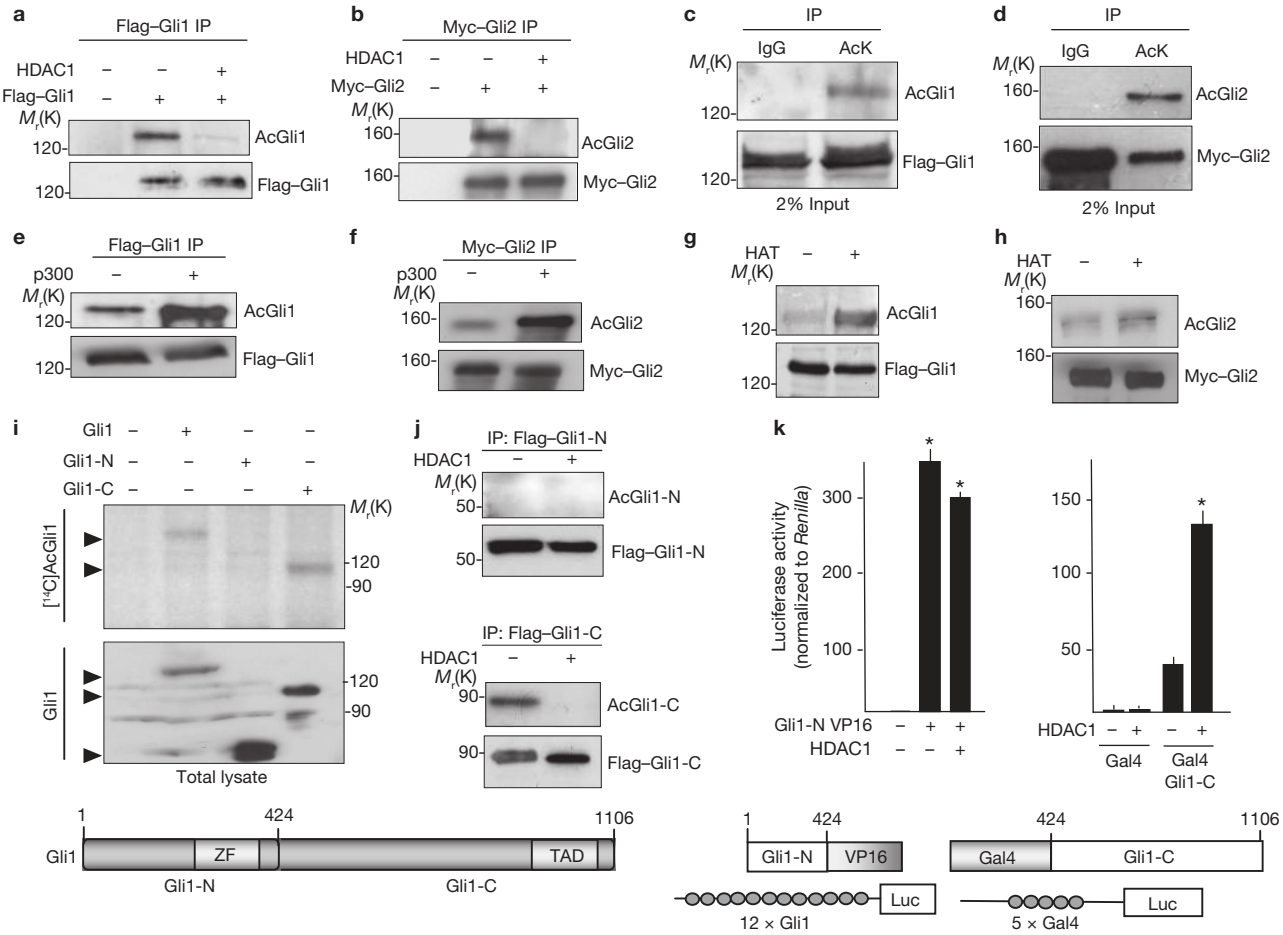

Figure 2 Gli1 and Gli2 are acetylated and deacetylated. (**a**–**f**) HEK293T cells were transfected with Flag–Gli1 (**a**, **c**, **e**), Myc–Gli2 (**b**, **d**, **f**), HA–HDAC1 (**a**, **b**) or HA p300 (**e**, **f**). After Flag (**a**, **e**), Myc (**b**, **f**), acetylated lysine or IgG (**c**, **d**) immunoprecipitation, acetylated Gli1 (AcGli1) and Gli2 (AcGli2) were detected by anti-acetylated lysine (**a**, **b**, **e**, **f**), anti-Flag (**c**) or anti-Myc (**d**) antisera. (**g**, **h**) Gli1 and Gli2 are acetylated *in vitro*. Purified Flag–Gli1 (**g**) or Myc–Gli2 (**h**) were incubated for 1 h with GST–HAT and their acetylation was revealed with an anti-acetylated lysine antibody. The same filters were re-probed with anti-Flag (**g**) or anti-Myc (**h**) antisera. (**i**) Top, *in vitro* [^{14}C] acetyl-CoA labelling. Purified Flag–Gli1 full-length, N-terminal (Gli1-N) or C-terminal (Gli1-C) regions were incubated with GST–HAT and [^{14}C] acetyl-CoA, subjected to SDS–PAGE and revealed by fluorography. Bottom, schematic representation of Gli1 N-terminal and C-terminal domains (ZF, zinc finger region; TAD, transcriptional activation domain). (**j**) *In vivo* acetylation of Gli1 N-terminal and C-terminal domains. HEK293T cells were transfected with Flag–Gli1-N or -C vectors with or without HA–HDAC1 and processed as described in **a**. (**k**) The activity of the C terminus, but not of the N terminus, of Gli1 is enhanced by HDAC1. Left, luciferase activity in HEK293T cells transfected with a plasmid encoding Gli1-N (amino acids 1–424)-VP16 and 12 × Gli–Luc reporter, alone or with HDAC1. Right, Gli1-C (amino acids 424–1106) fused to the Gal4 DNA-binding domain expression plasmid was transfected with a Gal4-responsive luciferase reporter for 24 h, in the absence or presence of HDAC1. Results are shown as the mean ± s.d. ($n = 3$). $^*P < 0.01$, versus control. Bottom, schematic representation of the Gli1-N VP16 and Gal4 Gli1-C constructs and reporters used. For uncropped images of blots, see Supplementary Information, Fig. S8.

agonist SAG[17] or Shh in a dose- and time-dependent manner (Fig. 1a and Supplementary Information, Fig. S1B–D), whereas other inhibitors (class III Sirt1 inhibitor sirtinol and class II HDAC6 inhibitor tubacin) were ineffective (Fig. 1a). In contrast, TSA, HDiA and HDiB treatment did not affect the activity of the MMP-1 promoter, an AP-1 target[18] (Supplementary Information, Fig. S1E). Accordingly, short interfering RNA (siRNA)-mediated depletion of class I HDAC1, but not class II HDAC4, significantly reduced *Gli1* mRNA levels (a readout of Hh signalling) in SAG-induced NIH 3T3 cells (Fig. 1b). Consistent with this, HDAC1 and HDAC2, but not Sirt1 overexpression, potentiated both basal and Gli1- and Gli2-mediated, but not Gli3-mediated, transcription (Fig. 1c and data not shown), indicating that class I HDACs are positive modulators of the activatory members of the Gli family.

The effect of HDACs on Gli function suggested a physical association. Indeed, endogenous HDAC1 and Gli1 formed a complex (Fig. 1d) and ectopic HDAC1 and HDAC2 co-immunoprecipitated with Gli1 (Fig. 1e, f) and Gli2 (Fig. 1g). To determine the occupancy of the Gli–HDAC complex on Gli-target genes (that is, *Ptch1*, whose transcription is activated by SAG and inhibited by co-treatment with TSA; Fig. 1h) we performed chromatin immunoprecipitation (ChIP) assays. HDAC1 or HDAC2 and Gli1 were recruited to the *Ptch1* promoter upon SAG treatment (Fig. 1i). The recruitment of these proteins as a complex was indicated by re-ChIP experiments, in which immunoprecipitated HDAC–chromatin complexes were subjected to a second round of immunoprecipitation with an anti-Gli1 antibody (Fig. 1j). Remarkably, SAG-induced HDAC–Gli1 recruitment was accompanied by hyperacetylation of histones H3 and H4 (Fig. 1i, j), suggesting that

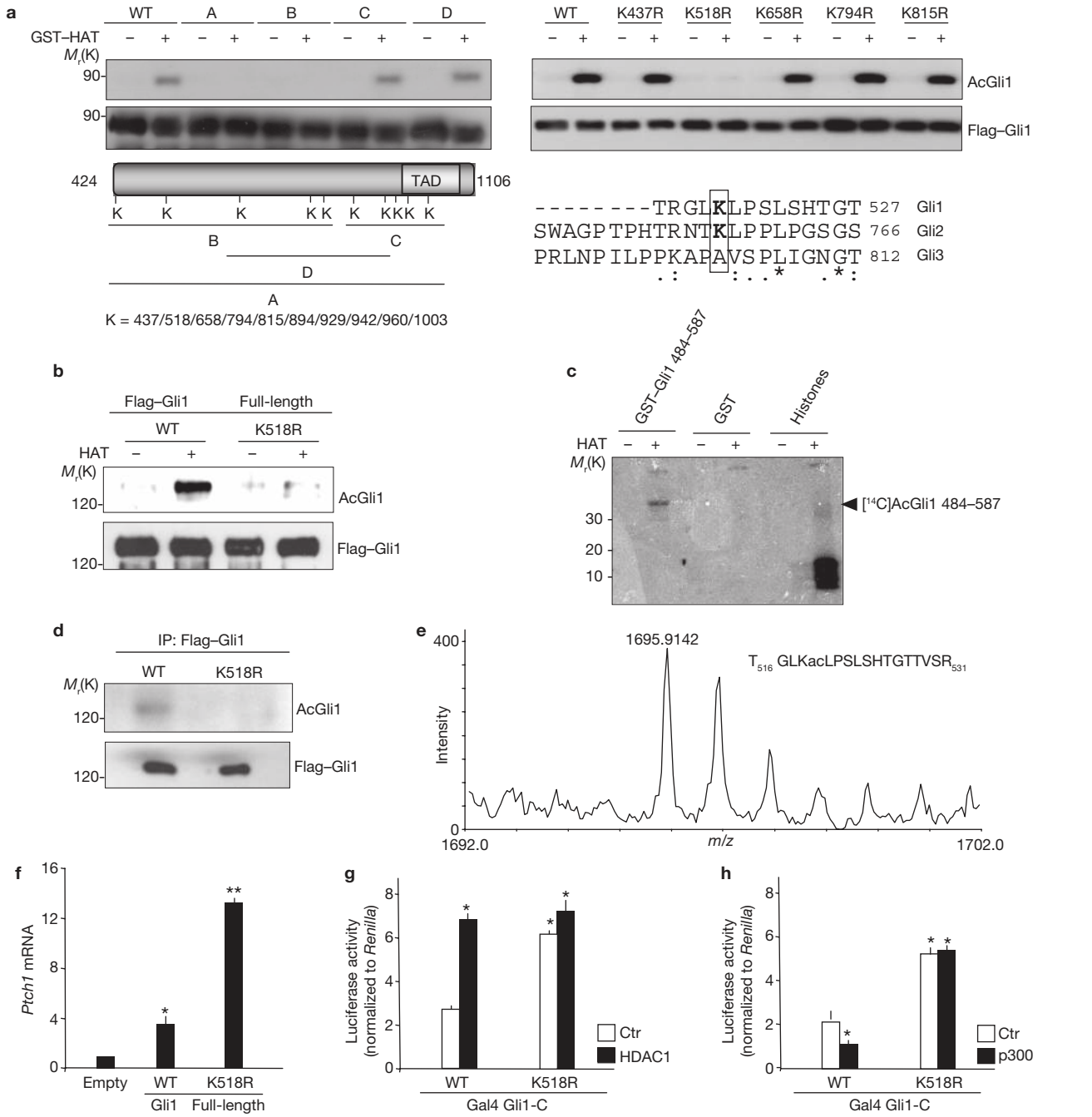

Figure 3 Gli1 is acetylated at Lys 518 *in vitro* and *in vivo*. (**a**) Left, Flag–Gli1-C terminus proteins containing all ten lysines and three different clusters of five lysines (A–D, shown in the bottom scheme) mutated to arginine, were expressed in HEK293T cells and purified. A HAT assay was performed as described in Fig. 2g. TAD, transcriptional activation domain. Top right, HAT assay of five single point mutants (K437R, K518R, K658R, K794R and K815R). Bottom right, ClustalW alignment of human Gli1, Gli2 and Gli3 protein sequences in the region surrounding Gli1 Lys 518. Identical, strongly conservative and weakly conservative amino acids are indicated by asterisks, colons and dots, respectively, according to ClustalW convention. (**b**) Flag-tagged full-length Gli1 or the Gli1^{K518R} mutant were purified and incubated with acetyl-CoA, in the absence or presence of GST–HAT. Acetylation of Gli1 was revealed by western blotting with an anti-acetylated lysine antibody. (**c**) [^{14}C]acetyl-CoA labelling of Gli1 amino acids 484–587. GST–Gli1 484–587, GST alone or histones (5 μg of each) were incubated with recombinant GST–HAT (1 μg) and [^{14}C]acetyl-CoA. Incorporation of [^{14}C]acetate was revealed by SDS–PAGE and fluorography. (**d**) Flag-tagged Gli1 wild type, Gli1^{K518R} mutant and p300 were transfected in HEK293T cells and an assay was performed as described in Fig. 2e. (**e**) The MALDI-ToF spectrum of the Gli1 peptide mass fingerprint focused in the range 1690–1700 to highlight the tryptic peptide $T_{516–531}$ (GLKacLPSLSHTGTTVSR, MH^+ at *m/z* 1695.9142; theoretical molecular mass = 1695.9282). Flag–Gli1 was expressed in HEK293T cells as indicated above, Flag-purified, run on a gel and the Gli1 band was cut from the gel and processed via tryptic proteolysis. The peptide mixture was analysed by a high resolution MALDI-ToF mass spectrometer. (**f**) The effect of full-length Gli1 wild-type and Gli1^{K518R} mutant on endogenous *Ptch1* mRNA levels. NIH 3T3 cells were transfected with the indicated plasmids for 48 h and the levels of *Ptch1* mRNA were measured by quantitative PCR. $*P < 0.01$, wild type versus empty; $**P < 0.01$, Gli1^{K518R} versus wild type. (**g**–**h**) Effect of HDAC1 (**g**) or p300 (**h**) on Gal4-C-terminal Gli1 wild-type- or Gli1^{K518R} mutant-induced Gli–Luc activity in 293T cells. $*P < 0.05$, versus wild-type control. Results in **f**–**h** are shown as the mean ± s.d. ($n = 3$). Ctr, control. WT, wild type. For uncropped images of blots, see Supplementary Information, Fig. S8.

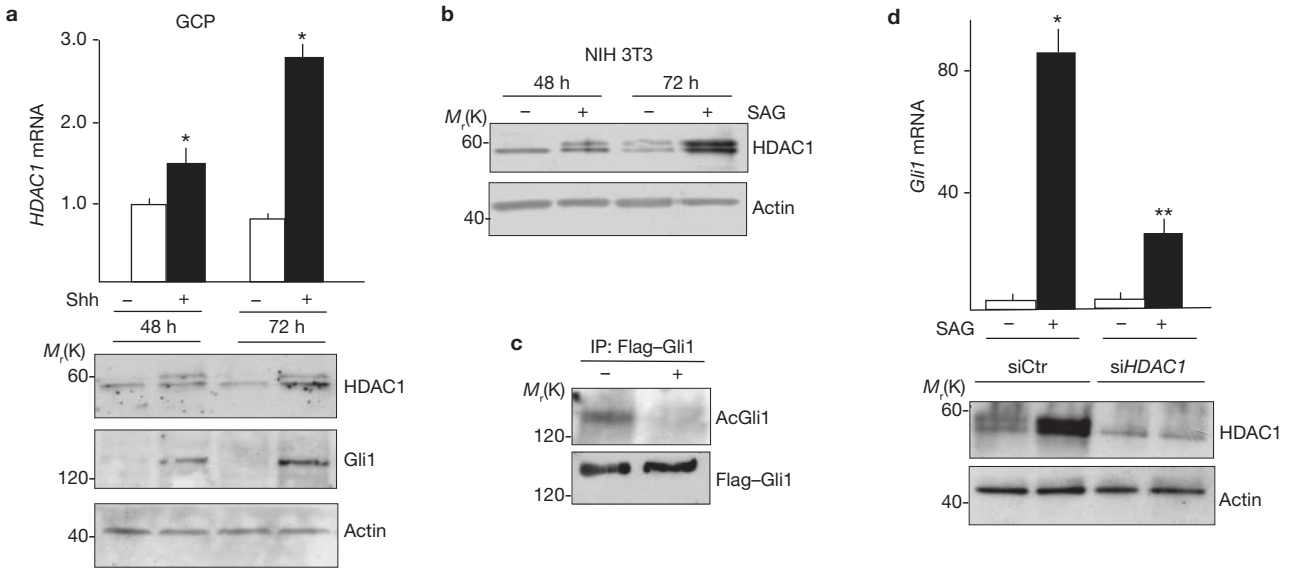

Figure 4 Shh promotes Gli1 activity by increasing HDAC1 levels. (**a**–**b**) Hh increases *HDAC1* mRNA (**a**) and protein levels (**a**, **b**) in cultured cerebellar GCPs (**a**) and NIH 3T3 cells (**b**). Cells were treated for the indicated times with Shh (**a**) or SAG (**b**). *HDAC1* mRNA levels were determined by quantitative PCR. Corresponding HDAC1, Gli1 and actin levels were analysed by western blotting analysis. $*P < 0.05$, versus untreated. (**c**) Hh activation promotes Gli1 deacetylation. NIH 3T3 cells were transfected with Flag–Gli1 and treated with SAG for 72 h. After Flag immunoprecipitation, Gli1 acetylation was revealed with an anti-acetylated lysine antibody. (**d**) Hh-induced activation of Gli function requires HDAC1. NIH 3T3 cells were transfected for 72 h with *HDAC1* siRNA or scrambled control and then treated for 72 h with SAG. *Gli1* mRNA (by quantitative PCR; top) and HDAC1 protein (bottom) levels at the end of the treatment. $*P < 0.01$, versus control; $**P < 0.01$ SAG + si*HDAC1* versus SAG alone. Results in **a** and **d** are shown as the mean ± s.d. ($n = 3$). Ctr, control. For uncropped images of blots, see Supplementary Information, Fig. S8.

the presence of HDAC during transcriptional activation was not related to histone deacetylation.

The Gli1 repressor Sufu (suppressor of fused) associates with SAP18 and mSin3, two members of the Sin3–HDAC co-repressor complex, recruiting them to Gli1 while TSA rescues the Sufu inhibitory effect, possibly through histone acetylation[19]. We therefore tested whether Sufu was involved in this context. Gli1 co-immunoprecipitated with HDAC1 in both control and Sufu-deficient cells and Sufu was not detected in the immunocomplexes (Fig S1f), demonstrating that this protein is not involved in the HDAC–Gli complex formation.

Gli1 acetylation at Lys 518 controls its transcriptional function

Activation of Gli1 is not linked to histone deacetylation, suggesting that HDAC1 may deacetylate Gli1 and Gli2. Indeed, anti-Gli1, anti-Gli2 or anti-acetylated lysine immunoprecipitates indicated that Gli1 and Gli2 are constitutively acetylated (Fig. 2a–d), that their acetylation is enhanced by p300-HAT (Fig. 2e, f) or by a recombinant HAT domain (GST–HAT; Fig. 2g, h) and that this is reverted by HDAC1 (Fig. 2a, b; Supplementary Information, Fig. S2A), *in vivo* and *in vitro*. [^{14}C]acetyl-CoA labelling of full-length Gli1 *in vitro* confirmed the incorporation of [^{14}C]acetate (Fig. 2i). Overall, these data demonstrate that Gli1 and Gli2 are acetylated *in vivo* and *in vitro*.

To investigate whether acetylation affects distinct Gli1 functional domains, we performed *in vitro* [^{14}C]acetyl-CoA labelling of either amino-terminal DNA binding (amino acids 1–424) or carboxy-terminal transactivating (amino acids 424–1106) regions (Fig. 2i, bottom). The Gli1 C terminus, but not the N terminus, incorporated [^{14}C]acetate *in vitro* (Fig. 2i) and was deacetylated by HDAC1 *in vivo* (Fig. 2j). Accordingly, HDAC1 potently enhanced the activity of the Gli1 C terminus fused to the Gal4 DNA-binding domain upon co-transfection with a Gal4–luciferase (Luc) reporter, whereas the activity of the Gli1 N terminus fused to the VP16 transactivation domain upon co-transfection with Gli–Luc was not regulated by HDAC1 (Fig. 2k). These findings indicate that the HDAC-responsive site of Gli1 is located on the C terminus.

To map the acetylated residue, we performed a HAT assay on purified Gli1 mutants harbouring either all ten C-terminal lysines mutated to arginine, or three different clusters of five K to R mutations (mutants A–D; Fig. 3a, bottom left). Mutant A (Fig. 3a, left; Supplementary Information, Fig. S2B, C) and mutant B (Fig. 3a, left) were not acetylated, indicating cluster B lysines (437–815) as the acetylatable residues. Site-directed mutagenesis on each lysine of cluster B, revealed that Lys 518 is the only acetylatable residue (Fig. 3a, right, b). Accordingly, a GST–Gli1 polypeptide (amino acids 484–587) containing only Lys 518, specifically incorporated [^{14}C]acetate *in vitro* (Fig. 3c). This data was confirmed by mass spectrometry analysis (Supplementary Information, Fig. S2D), which showed that GST–Gli1 had a HAT-induced relative molecular mass (M_r) increment of 42. Moreover, the Gli1^{K518R} mutant failed to be acetylated *in vivo* (Fig. 3d) and mass spectrometry analysis of Gli1, purified from mammalian cells, identified the tryptic peptide encompassing the region 516–531 (Fig. 3e) as acetylated, further confirming that Lys 518 is acetylated *in vivo*. Interestingly, the region surrounding Lys 518 was conserved in Gli2, but not Gli3 (Fig. 3a, bottom right).

Remarkably, the non-acetylatable full-length Gli1^{K518R} mutant robustly enhanced endogenous *Ptch1* expression and the induction was significantly higher than that obtained with wild-type Gli1 (Fig. 3f). Accordingly, the transcriptional activity of the non-acetylatable Gli1^{K518R} C terminus, was significantly increased compared with wild-type Gli1 and was no longer enhanced by HDAC1 or inhibited by p300 (Fig. 3g, h), demonstrating the functional relevance of Lys 518 acetylation and the specificity of HDAC and HAT effects on Gli1.

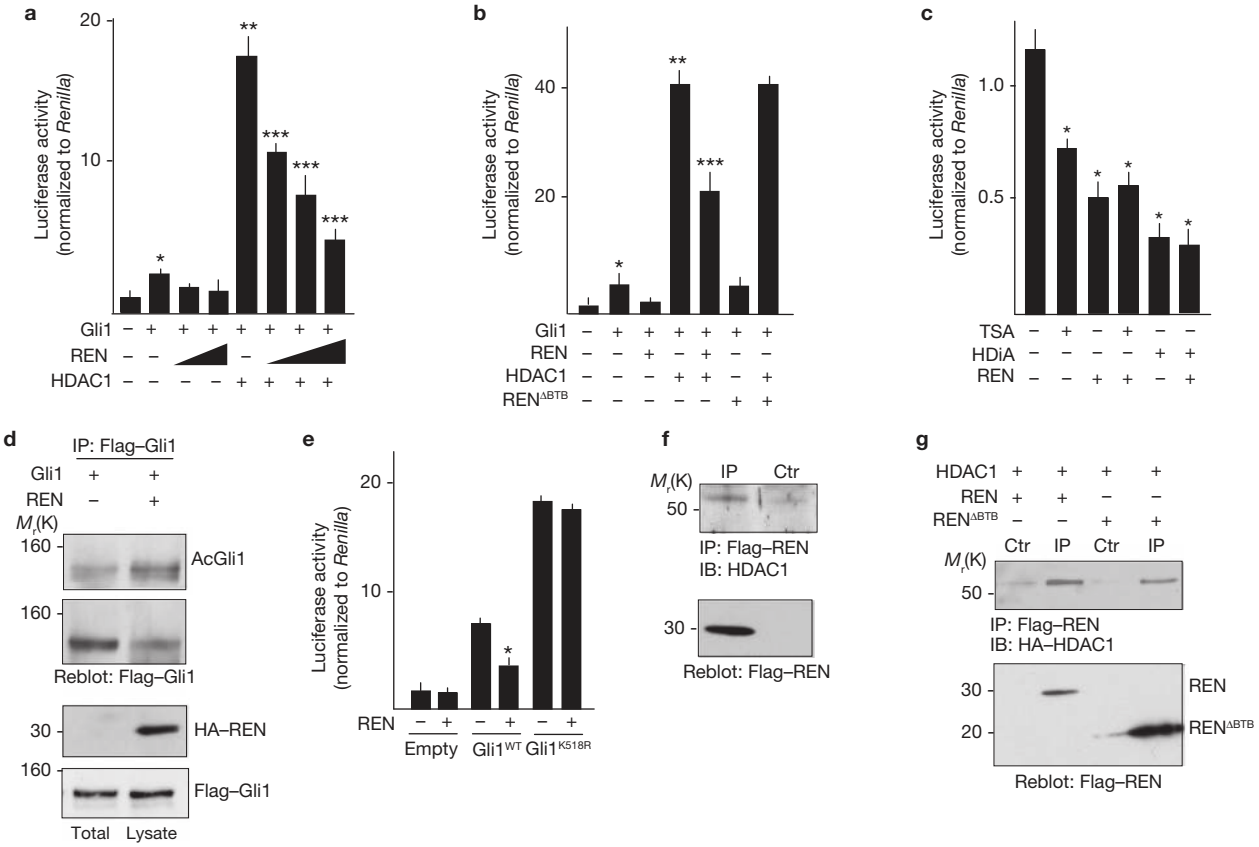

Figure 5 REN inhibits HDAC1 activity. (**a**, **b**) REN inhibits the Gli1-mediated transcriptional activation induced by HDAC1. Luciferase activity of HEK293T cells co-transfected with Gli–Luc and the indicated vectors (**a**; Gli1:REN ratios ranging from 1:0.125 to 1:1). $*P < 0.05$, Gli1 versus control; $**P < 0.05$, HDAC1 + Gli1 versus Gli1; $***P < 0.05$, REN + HDAC1 + Gli1 versus HDAC1 + Gli1. (**c**) REN-induced Gli-antagonism requires HDAC activity. *Ptch1*$^{-/-}$ MEFs were co-transfected with REN and Gli–Luc and either untreated or treated for 24 h with TSA or HDiA (2 μM). $*P < 0.05$. (**d**) Gli1 acetylation in HEK293T cells transfected with Flag–Gli1 alone or in combination with HA–REN. After immunoprecipitation with an anti-Flag antibody, acetylated Gli1 was detected by western blotting with an anti-acetylated lysine antibody. The blot was reprobed with an anti-Flag–Gli1 antibody to detect immunoprecipitated Gli1. Bottom, REN and Gli1 levels in cell lysates. (**e**) REN does not inhibit the Gli1^{K518R} mutant. HEK293T cells were transfected with the indicated vectors and a luciferase assay was performed as described above. $*P < 0.01$. WT, wild type. (**f**, **g**) REN and the REN$^{\Delta BTB}$ mutant interact with endogenous (**f**) and exogenous (**g**) HDAC1. Anti-Flag immunoprecipitation of Flag–REN or Flag– REN$^{\Delta BTB}$ transfected in HEK293T cells with (**g**) or without (**f**) HA–HDAC1 and immunoblotting with the indicated antibodies. Negative controls were performed as described above. Results in **a**–**c** and **e** are shown as the mean ± s.d. ($n = 3$). Ctr, control. For uncropped images of blots, see Supplementary Information, Fig. S8.

Overall, these data identify Gli1 acetylation at Lys 518 as a transcriptional switch, where its HDAC-mediated deacetylation confers enhanced transcriptional activity.

Hh activation promotes Gli1 activity by increasing HDAC1 levels

As HDACs are critical mediators of Gli function, we next sought to understand how these enzymes are regulated and functionally connected to the Hh pathway. Treatment of GCPs with Shh increased the levels of both HDAC1 and Gli1 proteins and mRNAs (Fig. 4a) as well as proliferation rate, an effect antagonized by HDAC inhibition (Supplementary Information, Fig. S3A–C). Similarly, treatment of NIH 3T3 cells with SAG significantly increased the levels of HDAC1 protein (Fig. 4b), indicating that the effect is not cell restricted. Consistent with the HDAC1 increase, SAG treatment also resulted in Gli1 deacetylation (Fig. 4c). Importantly, the siRNA-mediated depletion of HDAC1 prevented the SAG-induced upregulation of the Gli target gene *Gli1* (Fig. 4d), demonstrating that the Hh-induced increase of HDAC1 levels is functionally relevant. These data strongly suggest the presence of a Hh-induced and HDAC-mediated positive autoregulatory loop of Gli function, in which, by increasing the levels of HDAC1, Hh triggers an auto-reinforcement mechanism of Gli transcriptional activity.

Negative regulation of HDAC1 by a Cul3–REN E3 ubiquitin ligase complex

A regulated extinction of Gli1 function is critical to ensure proper development and to prevent tumorigenesis. Having found that HDAC1 is a potent enhancer of Gli1 activity, we asked how this activation loop might be switched off and whether this mechanism may be deregulated in cancer.

In previous work we have found that REN, a BTB domain-containing protein encoded by a gene frequently deleted in medulloblastoma, inhibits Gli1-dependent transcription, thereby promoting growth arrest and differentiation of GCPs and medulloblastoma cells[15,20]. Therefore, we wondered whether REN could affect the HDAC-mediated activation of Gli1. Overexpressed REN, but not REN$^{\Delta BTB}$, a BTB domain-deleted mutant lacking Gli1 antagonistic activity, reverted the enhancing effect of ectopic HDAC1 upon Gli1-activated Gli–Luc (Fig. 5a, b).

To study the ability of REN and HDACi to counteract a constitutively activated endogenous Hh pathway we used the *ex vivo* model of

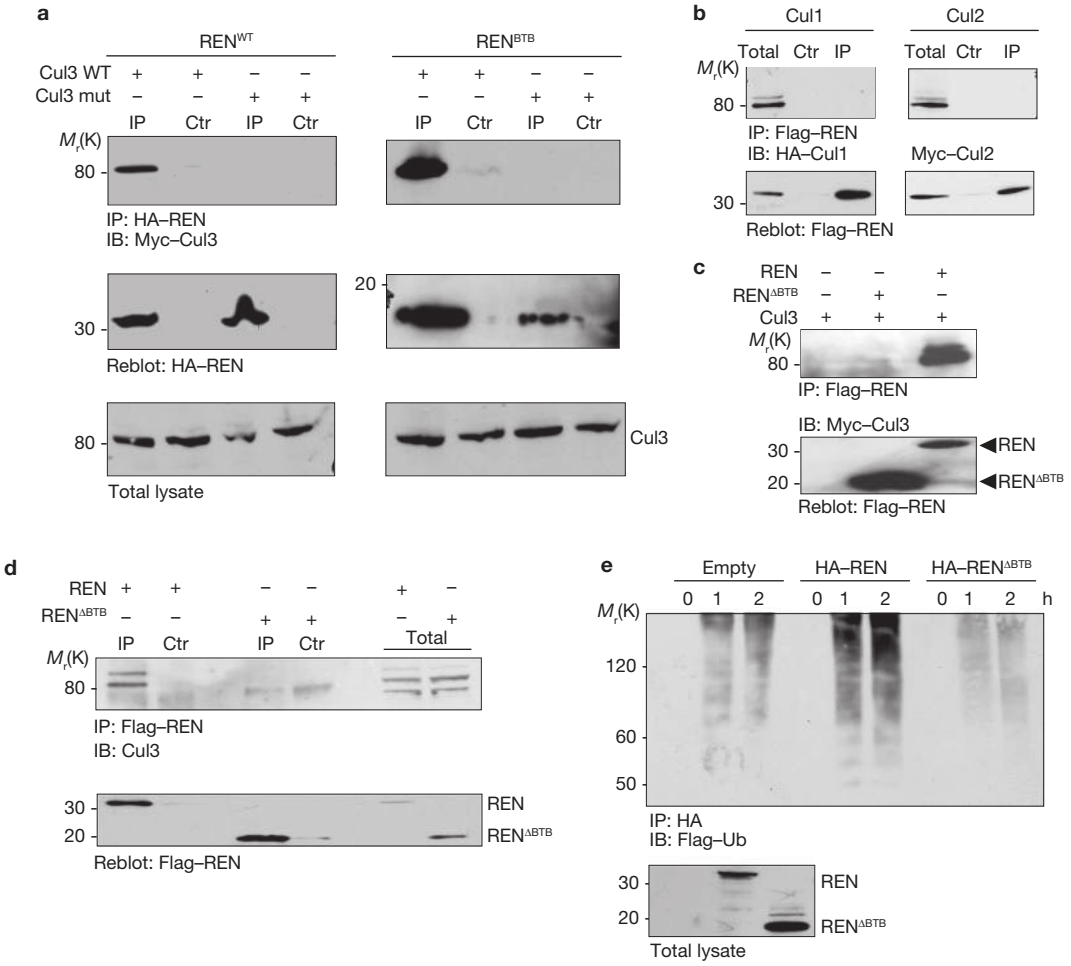

Figure 6 REN forms a ubiquitin ligase complex with Cul3. (**a**) REN associates with Cul3, but not with its mutant, Cul3 mut (Y58/62/125K; Supplementary Information, Figs S4 and S5). HEK293T cells were co-transfected with Myc–Cul3 wild type or Myc–Cul3 mut in the presence of HA–REN (WT, left) or the isolated REN^{BTB} mutant (HA–REN$^{\Delta BTB}$, right). Immunoprecipitation was carried out with an anti-HA antibody and immunocomplexes were revealed with an anti-Myc antibody. The blot was reprobed with an anti-HA antibody (reblot REN). Bottom, Cul3 and REN levels in total cell lysates. (**b**) REN does not interact with Cul1 or Cul2. HEK293T cells were co-transfected with Flag–REN and Myc–Cul2 or HA–Cul1. Immunoprecipitation was carried out as described in **a**. Immunocomplexes were revealed with anti-Myc or anti-HA antibodies. The blot was reprobed with an anti-Flag antibody to confirm REN immunoprecipitation. (**c**–**d**) Endogenous and exogenous Cul3 associates with REN, but not with its mutant REN$^{\Delta BTB}$. Anti-Flag immunoprecipitates of Flag–REN or Flag–REN$^{\Delta BTB}$ transfected in HEK293T cells with (**c**) or without (**d**) Myc–Cul3 and immunoblotting with anti-Myc (**c**) or anti-Cul3 (**d**) antibodies. The blots were reprobed with an anti-Flag antibody. (**e**) REN shows E3 ubiquitin ligase activity. HEK293T cells, transfected with an HA-tagged empty, REN or REN$^{\Delta BTB}$ vector were treated with MG132 (50 μM) 6 h before lysis. Immunoprecipitation was carried out with an anti-HA antibody and immunocomplexes were subjected to an *in vitro* ubiquitylation assay in the presence of Flag–ubiquitin (Flag–Ub) and immunoblotted with an anti-Flag antibody to detect proteins ubiquitylated by REN. Bottom, REN and REN$^{\Delta BTB}$ levels in total cell lysates. Ctr, control. WT, wild type. For uncropped images of blots, see Supplementary Information, Fig. S8.

Ptch$^{-/-}$ mouse embryonic fibroblasts (MEFs), in which *Ptch1* deletion causes constitutive Gli activation[21]. REN, HDiA and TSA inhibited the Hh-dependent activity of Gli–Luc and, most importantly, abrogation of HDAC function abolished REN-mediated suppression of Gli-induced transcription (Fig. 5c). Overall, these findings suggest that the ability of REN to inhibit HDAC function is required for its Hh antagonistic role.

The effect of HDAC on Gli1 function is mediated by its ability to modify Gli1 acetylation, suggesting that REN may lead to Gli1 hyperacetylation. Indeed, REN increased the acetylation status of Gli1 (Fig. 5d) and failed to inhibit the activity of the non-acetylatable Gli1^{K518R} mutant (Fig. 5e), suggesting that Gli1 acetylation represents the target of REN action through HDAC. Accordingly, endogenous (Fig. 5f) and exogenous (Fig. 5g) HDAC1 co-immunoprecipitated with REN, demonstrating that the two proteins form a complex. Surprisingly, the REN-BTB domain is not required for HDAC1 interaction (Fig. 5g), although is necessary to impair the effect of HDAC1 on Gli1, probably by recruiting an additional cofactor.

BTB domain-containing proteins belong to a family of adaptors recently shown to interact through their BTB domain with Cullin3 (Cul3), a component of the SCF-like E3 ubiquitin ligase complex[22]. To test whether REN may function as an adaptor, we studied its interaction with Cul3. REN or its BTB domain (REN^{BTB}) co-immunoprecipitated with ectopic or endogenous Cul3, but not with Cul1 or Cul2 (Fig. 6a, b). As expected, REN$^{\Delta BTB}$ did not bind ectopic (Fig. 6c) or endogenous (Fig. 6d) Cul3, indicating that the BTB domain is required for this interaction. Site-directed mutagenesis of residues predicted to be critical for Cul3–REN binding

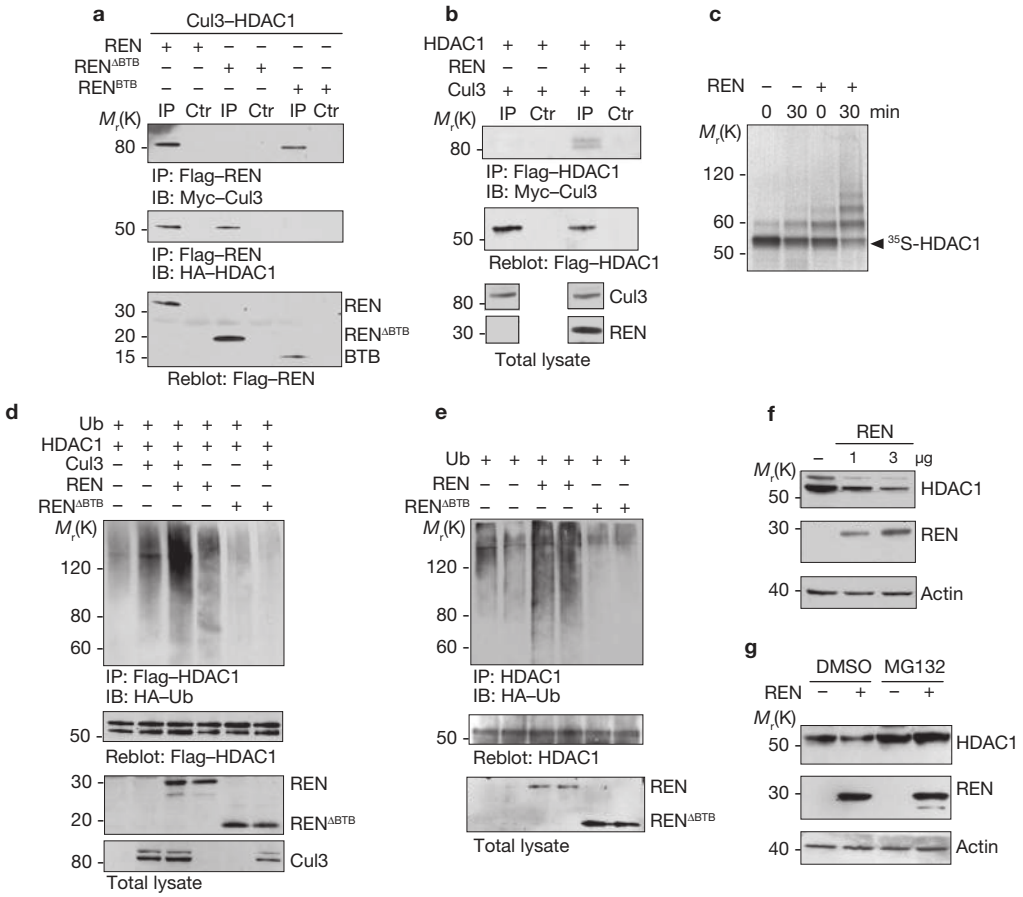

Figure 7 HDAC1 is ubiquitylated and negatively regulated by the Cul3–REN complex. (**a**) REN forms a complex with Cul3 and HDAC1. HEK293T cells were co-transfected with Flag–REN, Flag– $REN^{\Delta BTB}$ or Flag– REN^{BTB}, in the presence of HA–HDAC1 and Myc–Cul3. Immunoprecipitation was carried out as described in Fig. 6 and immunoblotting was performed with the indicated antibodies. (**b**) HDAC1 forms a complex with Cul3 only in the presence of REN. HEK293T cells were co-transfected with Flag–HDAC1 and Myc–Cul3 with or without HA–REN. Immunoprecipitation and immunoblotting were carried out as described in **a**. Bottom, Cul3 and REN levels in total cell lysates. (**c**) REN ubiquitylates HDAC1 *in vitro*. *In vitro*-translated ^{35}S-labelled HDAC1 was tested as described in the Methods, in the absence or presence of recombinant REN, for the indicated times. ^{35}S-labelled HDAC1 was revealed by SDS–PAGE and fluorography. (**d**, **e**) REN, but not $REN^{\Delta BTB}$, and Cul3 induce exogenous and endogenous HDAC1 ubiquitylation *in vivo*. Exogenous Flag–HDAC1 (**d**) or endogenous HDAC1 (**e**) were immunoprecipitated from MG132 (50 μM)-treated HEK293T cells expressing the indicated proteins, followed by western blotting with an anti-HA antibody to detect conjugated HA–ubiquitin (HA–Ub). The blot was reprobed with an anti-Flag–HDAC1 (**d**) or anti-HDAC1 (**e**) antibody. Bottom, REN, $REN^{\Delta BTB}$ and Cul3 protein levels in total cell lysates. (**f**) REN expression reduces the steady-state HDAC1 protein levels. HEK293T cells were transfected with HA–HDAC1 in the presence or absence of increasing amounts of Flag–REN and immunoblotted with anti-HA, anti-Flag or anti-actin antibodies. (**g**) HDAC1 is stabilized by MG132. HEK293T cells were transfected with HA–HDAC1 in the presence or absence of Flag–REN, and treated with or without MG132 (50 μM) before immunoblotting with anti-HA, anti-Flag and anti-actin antibodies. Ctr, control. For uncropped images of blots, see Supplementary Information, Fig. S8.

confirmed the specificity of the interaction (Fig. 6a; Supplementary Information, Figs S4 and S5). These data suggest that REN functions as an adaptor able to promote Cul3-dependent substrate ubiquitylation, thus representing an E3 ligase complex. Indeed, cell-purified REN (containing both the REN E3 ligase complex and associated substrates) showed protein ubiquitylation activity *in vitro,* whereas purified $REN^{\Delta BTB}$ was ineffective (Fig. 6e).

By adapting HDAC1 to Cul3, REN might lead to HDAC1 ubiquitylation. This was confirmed by the ability of REN to co-immunoprecipitate with Cul3 and HDAC1 together (Fig. 7a) and by the failure of HDAC1 to bind Cul3 in the absence of REN (Fig. 7b). Accordingly, recombinant HDAC1, was efficiently ubiquitylated *in vitro* in the presence of REN (Fig. 7c). Furthermore, overexpressed REN, alone or in combination with Cul3, promoted polyubiquitylation of exogenous or endogenous HDAC1, whereas REN mutants unable to bind Cul3 were ineffective, indicating that an intact Cul3–REN complex is required (Fig. 7d, e; Supplementary Information, Fig. S5D).

REN-induced HDAC1 ubiquitylation leads to the proteasome-mediated degradation of HDAC1, as indicated by the significant decrease of HDAC1 protein levels after the overexpression of increasing amounts of REN (Fig. 7f), an effect reverted by the proteasome inhibitor MG132 (Fig. 7g).

Conversely, REN was unable to bind Gli1 (Supplementary Information, Fig S6A), indicating that a direct association with the transcription factor is not involved in REN activity. REN also failed to promote ubiquitylation of, and to perturb levels of , Gli1 wild type or $Gli1^{K518R}$ mutant protein, whose stability was similar, both in the absence or presence of REN (Supplementary Information, Fig. S6B, D), demonstrating that Lys 518 acetylation and REN do not modify Gli1 stability.

Overall, these data suggest that REN suppresses Hh signalling through Cul3-mediated ubiquitylation and degradation of HDAC1.

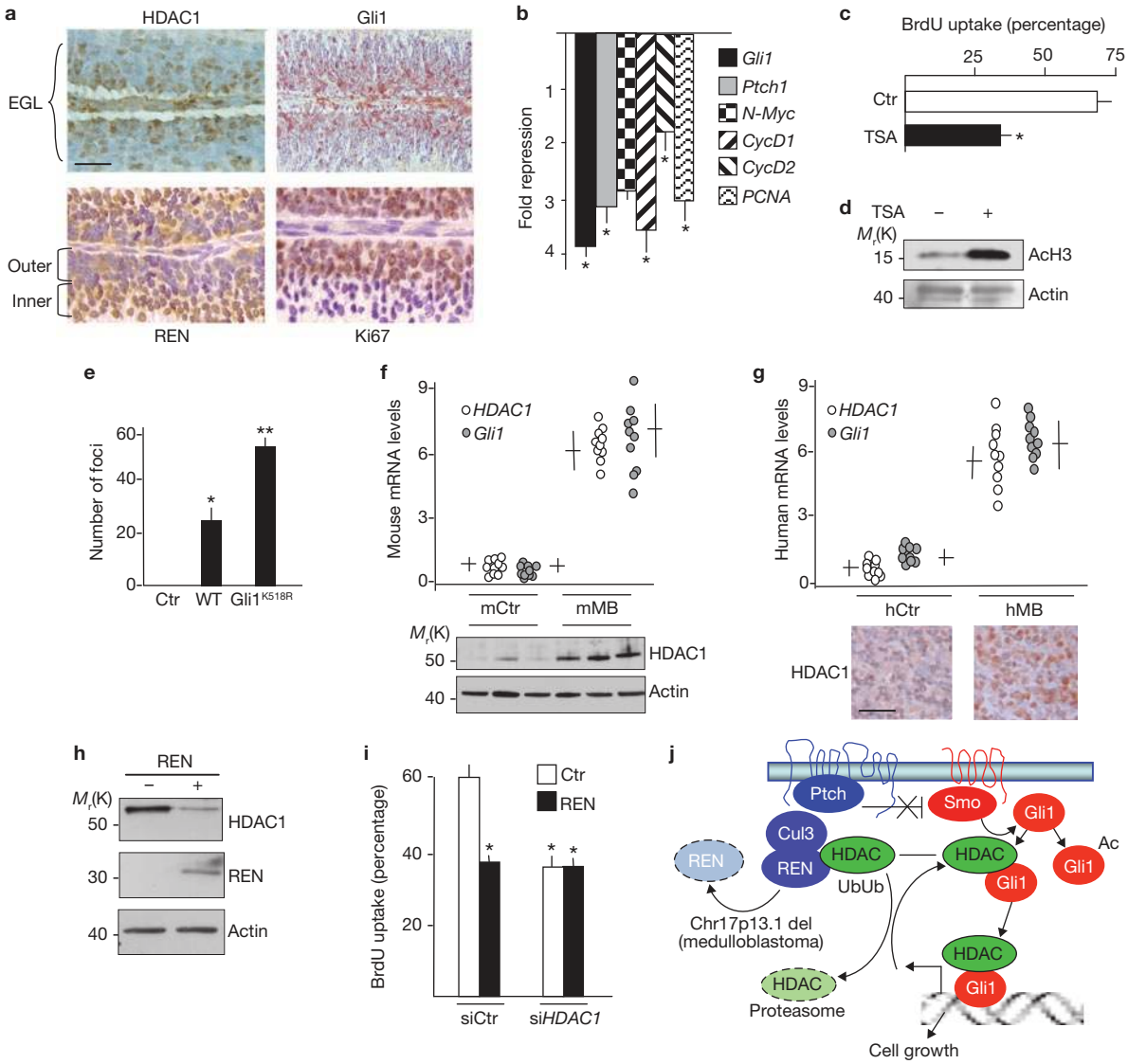

Figure 8 HDAC1 controls Hh-dependent GCP and medulloblastoma cell growth. (**a**) Immunohistochemical staining of HDAC1, Gli1 and Ki67 in the outer EGL, and of REN in the inner EGL, of a 4-day-old mouse cerebellum. Scale bar, 30 μm. (**b**–**d**) Three-day-old mice (four for each group) were injected subcutaneously with TSA (10 μg per g body weight) or DMSO. After 24 h, cerebellar GCPs were isolated to measure mRNA levels of the indicated targets by quantitative PCR (**b**), the percentage of BrdU incorporating cells (18 h BrdU labelling; **c**) and histone-H3 acetylation (AcH3) to monitor treatment efficacy (**d**). Fold repression in **b** was calculated by dividing DMSO-treated by TSA-treated mRNA values for each gene. $*P < 0.01$. (**e**) RK3E cells were transfected with Gli1 wild type (WT) or Gli1^{K518R} mutant, grown for three weeks and stained with crystal violet, and the number of transformed foci were counted. $*P < 0.05$, wild type versus control; $**P < 0.05$, Gli1^{K518R} versus wild type. (**f**) Levels of *HDAC1* and *Gli1* mRNAs (quantitative PCR) in mouse primary *Ptch1*$^{+/-}$medulloblastoma (mMB) versus normal cerebellum (mCtr). Bottom, western blot of HDAC1 levels in samples of mouse medulloblastoma versus normal cerebella. (**g**) Levels of *HDAC1* and *Gli1* mRNAs (quantitative PCR) in human primary medulloblastomas (hMB) versus normal cerebellum (hCtr). Bottom, immunohistochemistry of HDAC1 in human medulloblastoma versus normal cerebellum. Scale bar, 30 μm. (**h**) Daoy cells were transfected with HA–REN or control vector, and cell lysates were subjected to western blotting using anti-HDAC1, anti-HA or anti-actin (as loading control) antibodies. (**i**) Daoy cells were transfected with HDAC1or control siRNA for 72 h and then transfected again with REN for 48 h. BrdU uptake was assayed to monitor cell proliferation. $*P < 0.05$. (**j**) Model of the HDAC-dependent regulation of Gli1 activity. Gli1 binds and is deacetylated by HDAC1, which is recruited onto Hh target genes, possibly as a complex with Gli1, thus activating the transcription of cell-cycle genes. This event is switched off by degradation of HDAC1 through the ubiquitin ligase activity of the Cul3–REN complex. Loss of REN caused by chromosome 17p deletion, frequently observed in medulloblastoma, allows HDAC1 accumulation and enhancement of Hh signalling, thereby sustaining cell growth. Results in panels b, c, e, i, f and g are shown as the mean ± s.d. (panels b, c, e, i, f, n=3; panels f, g, $n=10$). Ctr, control. WT, wild type. For uncropped images of blots, see Supplementary Information, Fig. S8.

Control of Gli function by HDAC is required for GCP proliferation

Hh signalling is a critical regulator of GCP development and *in vitro* treatment of GCPs with HDACi suppressed both Shh-induced increase in proliferation rate and Gli1 mRNA and protein levels (Supplementary Information, Fig. S3A–C). Therefore, the HDAC-mediated positive and negative (REN) regulatory mechanisms described above, prompted us to investigate their role in Hh-dependent GCP growth *in vivo*. To this end, we first tested HDAC1 expression in GCPs at an early post-natal Hh-dependent developmental stage.

HDAC1 and Gli1 expression is correlated in developing cerebellum, as both are expressed predominantly in the Hh-dependent outer external germinal layer (EGL), where highly proliferating GCPs reside (Fig. 8a). In contrast, REN is localized only in non-proliferating inner EGL GCPs (Fig. 8a)[20], according to its ability to inhibit the Hh-dependent growth of GCPs[20]. These finding suggest that REN may withdraw Hh signalling by suppressing HDAC1 *in vivo*.

Conversely, the colocalization of HDAC1 and Gli1 in the outer EGL, suggests that, by enhancing Hh signalling, HDAC1 may control GCP proliferation. To test this hypothesis, we treated 4-day-old mice (when GCPs are actively proliferating under Shh stimulus) with TSA. Analysis of mRNA levels in GCPs isolated from killed mice revealed that Hh signalling was strongly inhibited in mice treated with TSA for 6 h and 24 h, compared with control-treated littermates, as several Gli-target genes were downregulated, including those involved in cell proliferation (for example, *Cyclins* and *N-Myc*; Fig. 8b; Supplementary Information, Fig S7A). Consistent with this, actively cycling BrdU (bromodeoxyuridine)-labelled GCPs from TSA-treated mice were drastically reduced compared with controls (Fig. 8c), according to the reduction of PCNA expression (Fig. 8b). The efficacy of the treatment was documented by histone H3 hyperacetylation in the cerebella of TSA-treated mice (Fig. 8d).

Overall, these data demonstrate that HDAC activity is critical for Hh-dependent GCP proliferation *in vivo* and *in vitro*.

HDAC1 is upregulated in medulloblastoma and is required for Hh-dependent regulation of tumour cell growth

As medulloblastoma arises from oncogenic transformation of GCPs aberrantly proliferating under Hh stimulation, we studied whether constitutive deacetylation of Gli1 is relevant for cellular transformation, by performing a transformation assay in rat kidney RK3E cells. As reported previously[3], ectopic expression of Gli1 induced foci formation (Fig. 8e, Supplementary Information, Fig. S7D). Notably, the Gli1^{K518R} mutant caused a significant increase in foci number compared with wild type Gli1, indicating that the deacetylation of Gli1 enhances its oncogenic activity.

To study whether Gli1 acetylation also affects medulloblastoma cell proliferation, we performed BrdU incorporation and MTS assays in D283 cells (an Hh-dependent medulloblastoma cell line originating from GCPs)[15], expressing ectopic wild-type Gli1 and the non-acetylatable Gli1^{K518R} mutant. Compared with control cells, wild-type Gli1 significantly increased BrdU incorporation and MTS conversion, which was further enhanced by the Gli1^{K518R} mutant (Supplementary Information, Fig. S7B, C), indicating that Lys 518 acetylation impairs cellular proliferation.

Based on the above data and on the failure of medulloblastoma to express the HDAC1 inhibitor REN[15], we hypothesized that upregulation of HDAC1 activity occurs in tumours. Indeed, significantly higher levels of HDAC1 and Gli1 were observed in mouse and human medulloblastoma tissue compared with normal tissue (Fig. 8f, g; Supplementary Information, Fig. S7E, F). Accordingly, abrogation of HDAC function by treatment of Hh-dependent medulloblastoma Daoy cells with a specific HDACi or suppression of endogenous HDAC1 levels by ectopic REN (Fig. 8h) or siRNA decreased both *Gli1* mRNA and proliferation levels[5,23] (Fig. 8i; Supplementary Information, Fig.S7G, H). In contrast, the REN-induced growth inhibitory effect was not observed after abrogation of HDAC function by HDiA or HDiB administration or *HDAC1* siRNA in Daoy cells (Fig. 8i; Supplementary Information, Fig. S7G), suggesting that HDAC activity is required to mediate the antiproliferative effect of REN, through impairment of Gli1 function.

Overall, our data indicate the relevance of HDAC-induced deacetylation of Gli1 in Hh-dependent medulloblastoma growth.

DISCUSSION

Here, we identify a mechanism whereby Hh signalling is regulated, in which acetylation of Gli1 at Lys 518 represents a transcriptional inhibitory switch, while its HDAC1-mediated deacetylation is responsible for transcriptional activation. This mechanism is the basis of a positive autoregulatory loop in which HDAC1 levels are increased by Shh. A similar mechanism may occur for Gli2, an early and essential transducer of post-receptor Hh signals, which shows a conserved region surrounding Lys 518 and is also deacetylated and enhanced by HDAC. Therefore, such an acetylation-deacetylation process is conserved in transcriptional activators of the pathway. A different acetylation-mediated mechanism seems to occur for Gli3, whose repressive transcriptional activity is attributed to the Ski-mediated interaction of its N terminus with HDAC, possibly leading to histone deacetylation[13]. Therefore, Hh signalling might undergo double acetylation-dependent control acting on chromatin histones or Gli transcription factors. Such a bifunctional role of HDAC would balance the activatory (Gli1 and Gli2) and inhibitory (Gli3) regulation of Hh signalling.

The coordinated pattern of expression of HDAC1, Gli1 and REN in different EGL GCP populations, suggests that HDAC1 is involved in Hh-dependent cerebellar development. Indeed, we show that TSA-induced withdrawal of HDAC function in mice impairs Hh activity and Hh-dependent growth of GCPs *in vivo*. Consistent with this, cerebellar development is impaired in HDAC1- and HDAC2-deficient mice[24] and pharmacological HDAC inhibition impairs neurogenesis in developing mouse embryos[25]. As HDACs also inhibit BMP 2-4 (an Hh antagonist) signalling[26,27], HDACs might also enhance Hh signalling through additional pathways. Furthermore, HDAC1 is required to maintain the Hh-dependent production of motoneurons during zebrafish neurogenesis[28], suggesting that this mechanism might be evolutionary conserved.

HDACs not only control developmental events (that is, differentiation, proliferation and apoptosis) but are also involved in diseases (for example, cancer)[8]. This highlights the relevance of physiological mechanisms that, by repressing HDAC function, prevent pathological consequences. We identify here a Cul3–REN E3 ubiquitin ligase complex, in which the newly discovered function of REN as a Cul3 adaptor leads to HDAC1 recruitment and degradation and, consequently, to Gli1 hyperacetylation and inhibition of its transcriptional activity. The ability of HDACi to suppress tumour growth is consistent with the role of *REN*, a tumour suppressor gene deleted in human medulloblastoma[15], in functioning as a native HDAC1 inhibitor, impairing cancer cell growth. Our data highlight the relevance of *REN* genetic loss in enhancing HDAC–Gli synergism in brain tumours, according to the emerging role of tumour suppressors whose genetic defects impair the HDAC-mediated control of tumorigenesis[29,30], a mechanism mimicked by therapeutic HDACi.

Therefore, the ability of HDAC1 to enhance Gli1 function, together with REN-mediated HDAC1 degradation, provide a model of an integrated mechanism involved in cerebellar development, whose deregulation may lead to Hh-dependent medulloblastoma growth, as a result of persistent Gli deacetylation (Fig. 8j). Indeed, the non-acetylatable Gli1^{K518R} mutant shows higher mitogenic and transforming activity

compared with wild-type Gli1 and high levels of both HDAC1 and Gli1 are also observed in primary medulloblastomas, which fail to express REN[15]. Overall, our observations provide a mechanistic explanation of the recent reports on the anti-tumour activity of HDACi treatment upon medulloblastoma in tumour-prone mice carrying loss of Ptch1 function or a gain-of-function mutation of Smo[31,32]. Accordingly, the HDAC inhibitor REN suppresses the *in vivo* growth of medulloblastoma xenografts by inhibiting Hh signalling[15].

Our findings are relevant for cancer therapy, as HDACs are druggable targets whose inhibition limits tumour growth through acetylation-dependent activation of tumour suppressor genes[8]. Conversely, we describe an alternative mechanism, where acetylation directly inhibits an oncogenic transcription factor (Gli1). Molecularly heterogeneous human medulloblastomas include a consistent Hh-dependent subgroup (about 50%)[5] carrying genetic alterations of *Ptch1*, *Smo* or *Sufu* and additional changes leading to Hh pathway activation. Although the therapeutic effectiveness of HDACi in Hh-independent medulloblastoma cannot be ruled out, through the targeting of additional oncogenic events, our data support the role of HDACi as promising agents for treatment not only of medulloblastoma but also of several additional tumours arising from canonical and non-canonical inappropriate activation of the Hh pathway[33], as suggested by their effects on pancreatic cancer[34].

In conclusion, REN-mediated negative and Hh-induced positive regulatory loops highlight the central role of Gli acetylation as a switch at the crossroads of ubiquitin-dependent inhibitory and deacetylation-mediated activatory mechanisms required for the fine-tuning of Hh signalling. □

METHODS

Methods and any associated references are available in the online version of the paper at http://www.nature.com/naturecellbiology/.

Note: Supplementary Information is available on the Nature Cell Biology website.

ACKNOWLEDGEMENTS

We thank M. P. Scott for the gift of *Ptch1*$^{-/-}$ cells, G. Giannini and M. Levrero, for helpful suggestions, L. Di Magno, M. Della Guardia, C. Fragomeli and D. Mazzà for experimental support. This work was supported by the Associazione Italiana per la Ricerca sul Cancro, Telethon Grant GGP07118, the Ministry of University and Research (FIRB and PRIN), the Ministry of Health, the Fondazione Roma Foundation, the Mariani Foundation, the Cenci-Bolognetti Foundation and the Rome Oncogenomic Center.

AUTHOR CONTRIBUTIONS

G.C. and L.D.M. designed and performed experiments, analysed data and wrote the paper; A.G., S.C., L.A., P.I., L.P., E.M., M.P., G.D.S., E.M.P., P.G. and A.G. performed experiments; E.D.S., E.F., C.S., L.V., C.P., M.E.S. and I.S. analysed data; A.G. designed experiments, analysed data and wrote the paper.

COMPETING FINANCIAL INTERESTS

The authors declare no competing financial interests.

Published online at http://www.nature.com/naturecellbiology/.
Reprints and permissions information is available online at http://npg.nature.com/reprintsandpermissions/.

1. Ruiz i Altaba, A. *Hedgehog-Gli Signaling in Human Diseases* (Plenum, 2006).
2. Jiang, J. & Hui, C. C. Hedgehog signaling in development and cancer. *Dev. Cell* **15,** 801–812 (2008).
3. Ruppert, J. M., Vogelstein, B. & Kinzler, K. W. The zinc finger protein GLI transforms primary cells in cooperation with adenovirus E1A. *Mol. Cell Biol.* **11,** 1724–1728 (1991).
4. Kimura, H., Stephen, D., Joyner, A. & Curran, T. Gli1 is important for medulloblastoma formation in *Ptc1+/–* mice. *Oncogene* **24,** 4026–4036 (2005).
5. Ferretti, E. *et al.* Concerted microRNA control of Hedgehog signalling in cerebellar neuronal progenitor and tumour cells. *EMBO J.* **27,** 2616–2627 (2008).
6. Huntzicker, E. G. *et al.* Dual degradation signals control Gli protein stability and tumor formation. *Genes Dev.* **20,** 276–281 (2006).
7. Di Marcotullio, L. *et al.* Numb is a suppressor of Hedgehog signalling and targets Gli1 for Itch-dependent ubiquitination. *Nature Cell Biol.* **8,** 1415–1423 (2006).
8. Minucci, S. & Pelicci, P. G. Histone deacetylase inhibitors and the promise of epigenetic (and more) treatments for cancer. *Nature Rev. Cancer* **6,** 38–51 (2006).
9. Glozak, M. A., Sengupta, N., Zhang, X. & Seto, E. Acetylation and deacetylation of non-histone proteins. *Gene* **363,** 15–23 (2005).
10. Zupkovitz, G. *et al.* Negative and positive regulation of gene expression by mouse histone deacetylase 1. *Mol. Cell Biol.* **26,** 7913–7928 (2006).
11. Yang, X. J. & Seto, E. The Rpd3/Hda1 family of lysine deacetylases: from bacteria and yeast to mice and men. *Nature Rev. Mol. Cell Biol.* **9,** 206–218 (2008).
12. Dai, P. *et al.* Sonic Hedgehog-induced activation of the Gli1 promoter is mediated by GLI3. *J. Biol. Chem.* **274,** 8143–8152 (1999).
13. Dai, P. *et al.* Ski is involved in transcriptional regulation by the repressor and full-length forms of Gli3. *Genes Dev.* **16,** 2843–2848 (2002).
14. Yoon, J. W. *et al.* GLI activates transcription through a herpes simplex viral protein 16-like activation domain. *J. Biol. Chem.* **273,** 3496–3501 (1998).
15. Di Marcotullio, L. *et al.* REN(KCTD11) is a suppressor of Hedgehog signaling and is deleted in human medulloblastoma. *Proc. Natl Acad. Sci. USA* **101,** 10833–10838 (2004).
16. Taipale, J. *et al.* Effects of oncogenic mutations in Smoothened and Patched can be reversed by cyclopamine. *Nature* **406,** 1005–1009 (2000).
17. Chen, J. K., Taipale, J., Young, K. E., Maiti, T. & Beachy, P. A. Small molecule modulation of Smoothened activity. *Proc. Natl Acad. Sci. USA* **99,** 14071–14076 (2002).
18. Canettieri, G. *et al.* The coactivator CRTC1 promotes cell proliferation and transformation via AP-1. *Proc. Natl Acad. Sci. USA* **106,** 1445–1450 (2009).
19. Cheng, S. Y. & Bishop, J. M. Suppressor of Fused represses Gli-mediated transcription by recruiting the SAP18-mSin3 corepressor complex. *Proc. Natl Acad. Sci. USA* **99,** 5442–5447 (2002).
20. Argenti, B. *et al.* Hedgehog antagonist REN(KCTD11) regulates proliferation and apoptosis of developing granule cell progenitors. *J. Neurosci.* **25,** 8338–8346 (2005).
21. Goodrich, L. V., Milenković, L., Higgins, K. M. & Scott, M. P. Altered neural cell fates and medulloblastoma in mouse patched mutants. *Science* **277,** 1109–1113 (1997).
22. Pintard, L., Willems, A. & Peter, M. Cullin-based ubiquitin ligases: Cul3–BTB complexes join the family. *EMBO J.* **23,** 1681–1687 (2004).
23. Bar, E. E., Chaudhry, A., Farah, M. H. & Eberhart, C. G. Hedgehog signaling promotes medulloblastoma survival via Bc/II. *Am. J. Pathol.* **170,** 347–355 (2007).
24. Montgomery, R. L., Hsieh, J., Barbosa, A. C., Richardson, J. A. & Olson, E. N. Histone deacetylases 1 and 2 control the progression of neural precursors to neurons during brain development. *Proc. Natl Acad. Sci. USA* **106,** 7876–7881 (2009).
25. Shaked, M. *et al.* Histone deacetylases control neurogenesis in embryonic brain by inhibition of BMP2/4 signaling. *PLoS One* **3**, e2668 (2008).
26. Zhao, H., Ayrault, O., Zindy, F., Kim, J. H. & Roussel, M. F. Post-transcriptional down-regulation of Atoh1/Math1 by bone morphogenic proteins suppresses medulloblastoma development. *Genes Dev.* **22,** 722–727 (2008).
27. Rios, I., Alvarez-Rodriguez, R., Martí, E. & Pons, S. Bmp2 antagonizes sonic hedgehog-mediated proliferation of cerebellar granule neurones through Smad5 signalling. *Development* **131,** 3159–3168 (2004).
28. Cunliffe, V. T. Histone deacetylase 1 is required to repress Notch target gene expression during zebrafish neurogenesis and to maintain the production of motoneurones in response to hedgehog signalling. *Development* **131,** 2983–2995 (2004).
29. Kim, J. E., Chen, J. & Lou, Z. DBC1 is a negative regulator of SIRT1. *Nature* **451,** 583–586 (2008).
30. Zhao, W. *et al.* Negative regulation of the deacetylase SIRT1 by DBC1. *Nature* **451,** 587–590 (2008).
31. Spiller, S. E., Ravanpay, A. C., Hahn, A. W. & Olson, J. M. Suberoylanilide hydroxamic acid is effective in preclinical studies of medulloblastoma. *J. Neurooncol.* **79,** 259–270 (2006).
32. Ecke, I. *et al.* Antitumor effects of a combined 5-aza-2'deoxycytidine and valproic acid treatment on rhabdomyosarcoma and medulloblastoma in *Ptch* mutant mice. *Cancer Res.* **69,** 887–895 (2009).
33. Scales, S. J. & de Sauvage, F. J. Mechanisms of Hedgehog pathway activation in cancer and implications for therapy. *Trends Pharmacol. Sci.* **30,** 303–312 (2009).
34. Chun, S. G., Zhou, W. & Yee, N. S. Combined targeting of histone deacetylases and hedgehog signaling enhances cytoxicity in pancreatic cancer. *Cancer Biol. Ther.* **8,** 1328–1339 (2009).

METHODS

Cell culture, plasmids, mutagenesis, drug treatments and antibodies. NIH 3T3, Shh light II, wild-type and *Ptch*$^{-/-}$ MEFs were cultured in DMEM plus 10% bovine serum; HEK293T, RK3E and Daoy cells, in DMEM plus 10% FBS; and D283 cells, in MEM plus 10% FBS. GCPs were isolated and cultured as described previously[20]. The following plasmids were provided by other laboratories: 8 × Gli–Luc (H. Sasaki, RIKEN Center for Developmental Biology, Japan), 12 × Gli–Luc (R. Toftgård, Karolinska Institutet, Sweden), pBJ5 HDAC1 and 2 (S. Shreiber, Harvard University, MA, USA), pcDNA3 Sirt1 (U. Jhala, University of California San Diego, CA, USA), pCMV-HDAC1 (P. L. Puri, The Burnham Institute, CA, USA), pcDNACul1, Cul2 and Cul3 (M. Pagano, New York University School of Medicine NY, USA), Myc–Gli2 (A. Dlugosz, University of Michigan, Ann Arbor, MI, USA), GST–HAT-pCAF and PCI-p300 (M. Fanciulli, Regina Elena Cancer Institute, Italy). PCR-amplified cDNAs of different human Gli1, REN^{KCTD11} and mutated forms were cloned into various tagged-vectors. Single or multiple residues were mutated by the Quickchange site-directed or multi-site mutagenesis kit (Stratagene).

Cell were treated with TSA (1 μM; Sigma), SAG (200 nM; Alexis) and Shh-N (3 μg ml^{-1}; R&D), unless otherwise specified. AcetylCoA was from Sigma, MG132 from Calbiochem and [^{14}C]acetyl-CoA from GE Healthcare.

Antibody sources and concentrations used were: rabbit polyclonal against acetylated lysine (western blotting 1:1,000; immunoprecipitation, IP, 1:100; Upstate), HDAC1 (western blotting 1:1,000 dilution; IP 1:250; ChIP 1:200; immunohistochemistry 1:100; Upstate) and acetyl histones H3 and H4 (western blotting 1:500; ChIP 1:200; Upstate), HDAC2 (1:1,000; Santa Cruz), HDAC4 (1:200; Santa Cruz) and Gli1 (western blotting 1:200; immuhistochemistry 1:100; Santa Cruz), Cul3 (1:500; Zymed/Invitrogen); mouse monoclonal against HA and Myc (western blotting 1:1,000; IP 1:500; Santa Cruz) and Flag (M2; western blotting 1:2,000; IP 1:200; Sigma); goat polyclonal against Gli1 (IP, 1:200; ChIP 1:400; Santa Cruz) and actin (1:1,000; Santa Cruz). Gli1 and other antibodies specificity was validated by siRNAs or microRNA methodologies and western blotting or immunohistochemistry, as described previously[5,7,20] (this study and manufacturers' instructions).

Transfections, and luciferase, proliferation and focus formation assays. Transfections were performed using Lipofectamine 2000 or Plus (Invitrogen). Luciferase and *Renilla* activity were assayed with a dual-luciferase assay system (Promega)[7]. Results are expressed as luciferase/*Renilla* ratios and represent the mean ± s.d. of at least three experiments, each performed in triplicate. Cell proliferation was evaluated by a BrdU-labelling assay (Roche)[15] or MTS-based proliferation assay system (Promega). Focus formation assays were carried out as described previously[18].

RNA interference and quantitative PCR. RNA knockdown was performed with pools of siRNA duplexes (50 to 100 nM) transfected with lipofectamine 2000. The following oligonucleotides were used: mouse *HDAC1* (Dharmacon), sense1 5′-ACACAGAGAUCCCUAAUGAUU-3′, antisense1 5′-PUCAUUAGGGAUCUCUGUGUUU-3′, sense2 5′-GAACUCUUCUAACUUCAAAUU-3′, antisense2 5′-PUUUGAAGUUAGAAGAGUUCUU-3′, sense3 5′-GGUAUUUGAUGGCUUGUUUUU-3′, antisense3 5′-PAAACAAGCCAUCAAAUACCUU-3′, sense4 5′-ACAAUUUGCUGCUCAACUAUU-3′, antisense4 5′-PUAGUUGAGCAGCAAAUUGUUU-3′; mouse *HDAC4*, sense1 5′-CAACAGGAGAUGCUGGCCAUU-3′, antisense1 5′-PUGGCCAGCAUCUCCUGUUGUU-3′, sense2 5′-GGCUCGGCCGCUCCACUUCUU-3′, antisense2 5′-PGAAGUGGAGCGGCCGAGCCUU-3′, sense3 5′-GAAAGGAGCCTGTGGCAACUU-3′, antisense3 5′-PGUUGCCUCUGGCUCCUUUCUU-3′.

Quantitative reverse transcription-PCR (RT-PCR) analysis of *Gli1*, *Ptch1*, *N-Myc*, *CycD1*, *CycD2*, *PCNA* and *HDAC1* mRNA was performed on cDNAs using the ABI Prism 7900HT Sequence Detection System (Applied Biosystems) employing both Assay on Demand Reagents and designed (HDAC1_mouse). The designed oligonucleotides used were as follows: *HDAC1*_M_Fow, 5′-TCGCTGCTGGACTTACGAAA-3′, *HDAC1*_M_Rev 5′-TGTAGGGCAGCTCATTAGGGA-3′. The Assay on Demand Reagents used for mouse samples were: *Gli1* (Mm00494645_m1), *Ptch1* (Mm00436026_m1), *N-Myc* (Mm00476449_m1), *CycD1* (Mm00432359_m1), *CycD2* (Mm00438071_m1), *PCNA* (Mm00448100_g1). The Assay on Demand Reagents used for human samples were: *Gli1* (Hs00171790_m1), *HDAC1* (Hs00606262_g1).

Each amplification reaction was performed in triplicate, and the average of the three threshold cycles was used to calculate the amount of transcript in the sample (SDS software, ABI). mRNA quantification was expressed in arbitrary units, as the ratio of the sample quantity to the calibrator or to the mean values of controls samples. All values were normalized to two endogenous controls: HPRT (Mn00446968_m1) and β2microglobulin (Mn00437762_m1) for mouse samples, β-actin (4326315E-0506007) and HPRT (4326321E-0501006) for human samples.

Biochemical methods. Extract preparation, immunoprecipitation and immunoblotting were performed as described previously[7,35]. For acetylation assays, HEK293T or NIH 3T3 cells were transfected with the indicated plasmids and cell lysates were immunoprecipitated with specific antibodies (anti-acetyl-lysine, anti-Flag or anti-myc). In the experiments where immunoprecipitates were performed with an anti-acetylated lysine antibody or in the *in vivo* ubiquitylation assays, cells were first lysed with denaturing buffer (1% SDS, 50 mM Tris at pH 7.5, 0.5 mM EDTA, 1 mM DTT)[36,37] to disrupt protein–protein interactions, and then the lysates were diluted 10 times with lysis buffer and subjected to immunoprecipitation.

In vitro acetylation was carried out as described previously[38], using Flag–Gli1 and its mutants or Myc–Gli2 (transfected in HEK293T cells and purified by immunoaffinity chromatography) and GST–HAT-pCAF (purified from *E.Coli*) for 1 h. *In vitro* HDAC assay was performed by adding immunoaffinity chromatography-purified Flag–HDAC1 from HEK293T cells, to the *in vitro* acetylated Gli1 for 6 h, as described previously[35].

In vitro ubiquitylation was performed as described previously[39], by incubating either lysates from cells transfected with the indicated vectors or *in vitro* translated proteins, at 30 °C with 50 mM Tris-HCl at pH 7.5, 5 mM $MgCl_2$, 200 μM okadaic acid, 2 mM ATP, 0.6 mM DTT, 1 mM ubiquitin aldehyde, E1, Ubc3, Ubc5 and Flag–Ubiqutin. Flag–polyubiquitylated products were subjected to SDS–PAGE and immunoblotting.

To perform mass spectrometry analysis of *in vivo* acetylated full-length Gli1, Flag tagged Gli1 was expressed in HEK293T cells with p300 and then purified by Flag immunoaffinity chromatography and run on SDS–PAGE. The corresponding band was cut from the gel and processed via tryptic proteolysis. The peptide mixture was analysed by MALDI-ToF mass spectrometry and the resulting peptide mass fingerprint (PMF) used to identify proteins and determine their possible post-translational modifications by Mascot search engine.

Chromatin immunoprecipitation (ChIP) and Re-ChIP. ChIP was performed as described previously[18]. For ReChIP, the first chromatin immunocomplexes were eluted with 10 mM DTT and subjected to a second immunoprecipitation with control or specific antibodies as indicated. Eluted DNA was analysed with standard PCR techniques.

Oligonucleotides used for PCR amplification were: *Ptch1* promoter, forward 5′-GAGCATTCCTTAATGGAAG-3′, reverse 5′-CTGCAACGCGATTGGCTCT-3′; *GAPDH* Control: forward 5′-GACGGCCGCATCTTCTTGT-3′, reverse 5′-CCTGGTGACCAGGCGC-3′.

Immunohistochemistry. Sections from paraffin-embedded tissues were subjected to immunohistochemistry with the indicated primary antibodies[7,20]. Rabbit anti-HDAC1 (1:100 dilution in PBS/1% BSA) was used after protease digestion and incubated overnight at 4 °C.

Statistical analysis. StatView 4.1 software (Abacus Concepts) was used to perform statistical analysis. Results are expressed as the mean ± s.d. from an appropriate number of experiments as indicated in the figure legends. Statistical differences were analysed with the Mann-Whitney *U* test for non-parametric values and a $P < 0.05$ was considered significant.

HDAC activity assays and determination of inhibition profile of small molecule HDAC inhibitors. The inhibition profile of the small molecule HDAC inhibitors HDiA and HDiB on the activity of HDACs 1, 2, 3, 4, 5, 6, 7 and 8 was performed as described previously[40].

Mass Spectrometry. The molecular mass of recombinant GST–Gli1 (484–587) treated and untreated with HAT were determined by electrospray mass spectrometry (ES/MS) on a quadrupole mass spectrometer (Quattro micro Waters) equipped with HP 1100 HPLC (Agilent Technologies) using a C4 narrow bore reverse-phase column (Phenomenex 250 × 2.00 mm) at a flow rate of 200 ml min^{-1}. Mobile phase was 5% formic acid, 0.05% trifluoroacetic acid (eluent A) and 5%

DOI: 10.1038/ncb2013

formic acid, 0.05% trifluoroacetic acid in acetonitrile (eluent B) and a gradient of eluent B from 20% to 70% over 50 min was applied.

For analysis of *in vivo* acetylated full-length Gli1, the selected band was manually excised from gel and submitted to trypsin proteolysis. Briefly, after one destaining step using 50 mM ammonium bicarbonate (15 min), 50% acetonitrile in 50 mM ammonium bicarbonate (10 min) and 100% acetonitrile (15 min), about 100 ng of trypsin (Trypsin Gold, mass spectrometry grade, Promega), solubilised in 10 µl of a 25 mM ammonium bicarbonate digestion buffer, was added to vacuum-dried gel. Digestion was performed at 37 °C overnight. An aliquot of the peptide mixture was mixed with the same volume of α-cyano-4-hydroxy-*trans*-cinnamic acid matrix solution (5 mg ml^{-1}) in 70% acetonitrile containing 0.1% TFA (v/v) and spotted onto an appropriate MALDI target plate. MALDI-ToF MS analyses were performed in a Voyager-DE STR instrument (Applied Biosystems) equipped with a 337-nm nitrogen laser and operating in reflector mode. Mass data were obtained by accumulating several spectra from laser shots with an accelerating voltage of 20 kV. Two tryptic autolytic peptides were used for the internal calibration (*m/z* 842.5100 and 2807.3145).

The MS data were analysed by MoverZ program (v. 2002; http://bioinformatics.genomicsolutions.com), according to default parameters. Protein identification by peptide mass fingerprint (PMF), with the monoisotopic mass list, after exclusion of expected contaminant mass values by Peak Erazor program (http://www.protein.sdu.dk/gpmaw/Help/PeakErazor/peakerazor.html), was performed using the Mascot search engine (v. 2.2) against SwissProt database (v. 57.6, 495880 sequences; 174780353 residues). Up to one missed cleavage, 50 ppm measurement tolerance, oxidation at methionine and acetylation at lysine were considered. Identifications were validated when the probability-based Mowse protein score was significant according to Mascot[41].

Molecular modelling of Cul3 and REN interaction. To generate an atomic model of the interface between Cul3 and REN BTB, 3D models of the two proteins were created by homology modelling (Insight/Discover package, Biosym Technologies). Cul3 and REN BTB models were built using the crystallographic structures of Cul1 (PDB code 1LDK) and of Kv4.2 BTB domain (PDB code 1NN7), respectively. A Cul3–BTB REN complex was generated by considering the relative orientation of Cul1–Skp1 in the Cul1–Rbx1–Skp1–F box^{Skp2} SCF ubiquitin ligase complex[42]. The energy of this model was then minimized with the Insight/Discover package.

35. Canettieri, G. *et al.* Attenuation of a phosphorylation-dependent activator by an HDAC–PP1 complex. *Nature Struct. Biol.* **10,** 175–181 (2003).
36. Zhang, Q. *et al.* A hedgehog-induced BTB protein modulates hedgehog signaling by degrading Ci/Gli transcription factor. *Dev. Cell* **10,** 719–729 (2006).
37. Peschiaroli, A. *et al.* SCFβTrCP-mediated degradation of Claspin regulates recovery from the DNA replication checkpoint response. *Mol. Cell* **23,** 319–329 (2006).
38. Gu, W. & Roeder, R. G. Activation of p53 sequence-specific DNA binding by acetylation of the p53 C-terminal domain. *Cell* **90,** 595–606 (1997).
39. Zhao, X. *et al.* The HECT-domain ubiquitin ligase Huwe1 controls neural differentiation and proliferation by destabilizing the N-Myc oncoprotein. *Nature Cell Biol.* **10,** 643–653 (2008).
40. Lahm, A. *et al.* Unraveling the hidden catalytic activity of vertebrate class IIa histone deacetylases. *Proc. Natl Acad. Sci. USA* **104,** 17335–17340 (2007).
41. Pappin, D. J. Peptide mass fingerprinting using MALDI-TOF mass spectrometry. *Methods Mol. Biol.* **211,** 211–219 (2003).
42. Zheng, N. *et al.* Structure of the Cul1–Rbx1–Skp1–F box^{Skp2} SCF ubiquitin ligase complex. *Nature* **416,** 703–709 (2002).

nature cell biology

DOI: 10.1038/ncb2013

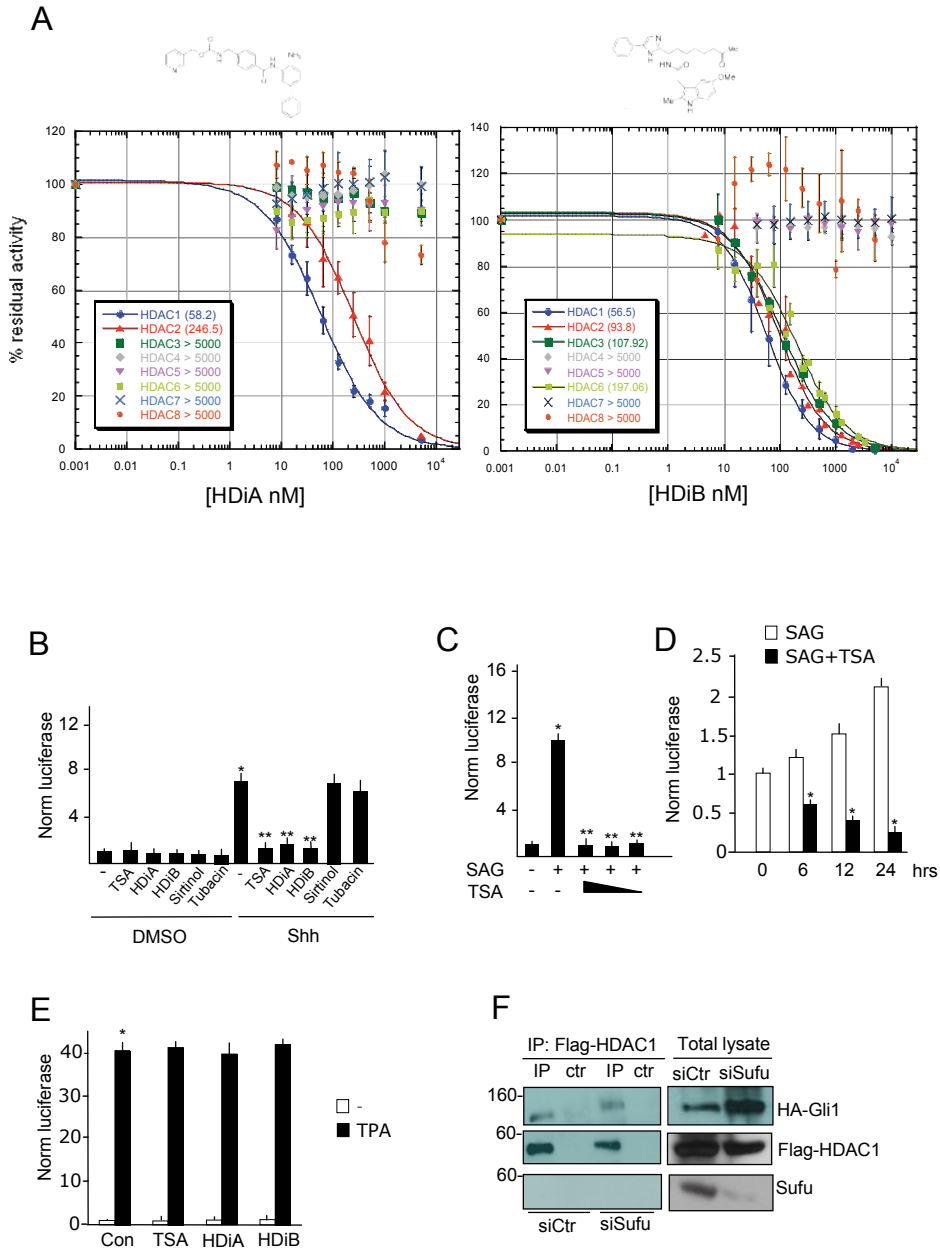

Figure S1 (**A**) Structure and dose-response curves of HDiA and HDiB showing the effect of both inhibitors on the activity of different HDACs. Activity of purified HDACs or HDAC complexes was measured with a fluorogenic assay as described in the Methods section. Enzymes were incubated with increasing concentrations of either compound in 9-point titration curves. Residual activity was determined with respect to a DMSO control and used to derive IC50 values. Results represents the average +/- SD of at least three separate experiments, each performed in triplicate. (**B**) Effect of HDACi on Shh-induced reporter activity. Shh light II cells we treated for 48h with Shh or DMSO, and for the last 24h with HDACi (1 microM TSA, 2 microM HDiA or HDiB, 25 microM sirtinol, 2.5 microM tubacin). * Shh vs control, p<0.01 ** Shh+HDACi vs Shh, p<0.05. (**C**) Dose response effect of TSA on Hh activity. NIH 3T3 Shh Light II cells were untreated or treated with 200 nM SAG alone or with decreasing amounts (1 to 0.1 microM) of TSA. * p<0.01, SAG vs untreated; ** p<0.01, SAG+TSA vs SAG alone. (**D**) Time course of the effect of TSA on Hh activity. Shh Light II were treated for 24h with SAG (200 nM) (0 time) and then treated with TSA (1 microM) or vehicle for the indicated times. * p<0.05, TSA+SAG vs SAG alone. (**E**) NIH 3T3 cells were transfected with MMP1-Luc, and renilla reporters and treated 10 hours with 1 microM TPA, 1microM TSA, 2microM HDiA or 2 microM HDiB, where indicated. * p<0.01 (**F**) Sufu is not necessary for the HDAC1/Gli1 binding. HEK293T cells were transfected with Sufu (siSufu) or scrambled (SiCtr) SiRNAs. After 72 hours from the first transfection, cells were transfected again with HA-Gli1 of Flag-HDAC1 plasmids for 24 hours. Immunoprecipitation was carried out as described with Flag antibody and the immunocomplexes revealed with the indicated antibodies. Results in panels b, c, d, e are shown as means ± s.d. (n=3).

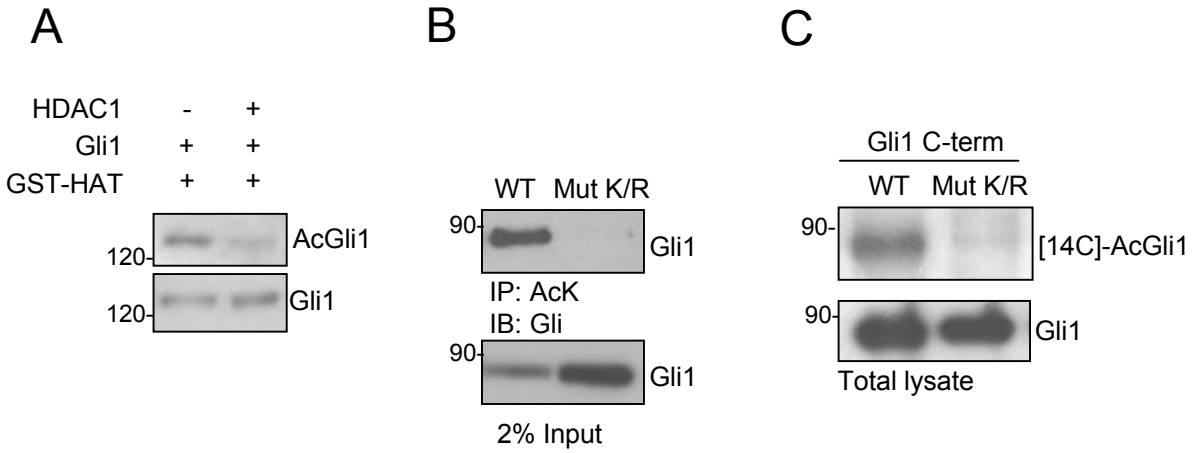

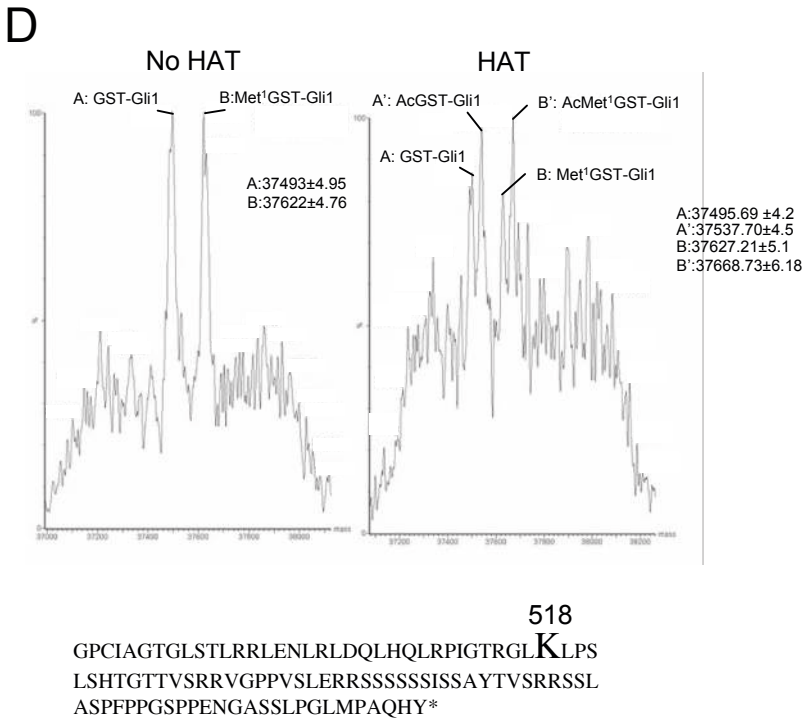

Figure S2 (**A**) Gli1 is deacetylated in vitro. Purified Flag-HDAC1 was incubated 6 hrs with purified and in vitro-acetylated Gli1 in 1X HDAC buffer (Upstate). Acetylated Gli1 was revealed with anti acetylated lysine antibody. (**B**) Plasmids encoding Flag-Gli1 C-terminal region or its mutant A, carrying K/R mutations of 10 lysine residues described in Figure 3A, were expressed in 293T cells. After trasfections, cells were lysed with a denaturing buffer and immunoprecipitated with anti-acetyl-lysine antibody. Western Blot was performed using anti-flag antiserum. (**C**) [^{14}C]-Acetyl-CoA labeling. Purified Flag-Gli1 C-term or its K/R mutant A was incubated with recombinant GST-HAT and [^{14}C]-Acetyl-CoA. Incorporation of [^{14}C]-Acetate by Gli1 was revealed by SDS Page and fluorography. (**D**) Electrospray mass spectrometry (ES/MS) analysis of GST-Gli1(484-587). Left Panel: Deconvoluted spectrum of recombinant GST-Gli1(484-587) showing two signals with an average molecular weight of 37493.89 ± 4.95 Da (A) and 37622.61 ± 4.76 Da (B), corresponding to protein species without and with Met1 respectively. Right Panel: Deconvoluted spectrum of recombinant GST-Gli1(484-587) treated with HAT, showing the 42 Da increment of protein species A (37495.69 ± 4.2) and B (37627.21 ± 5.1) to the average molecular weight of 37537.7 ± 4.5 Da (A') and 37668.73 ± 6.18 Da (B'), corresponding to mono-acetylated products.

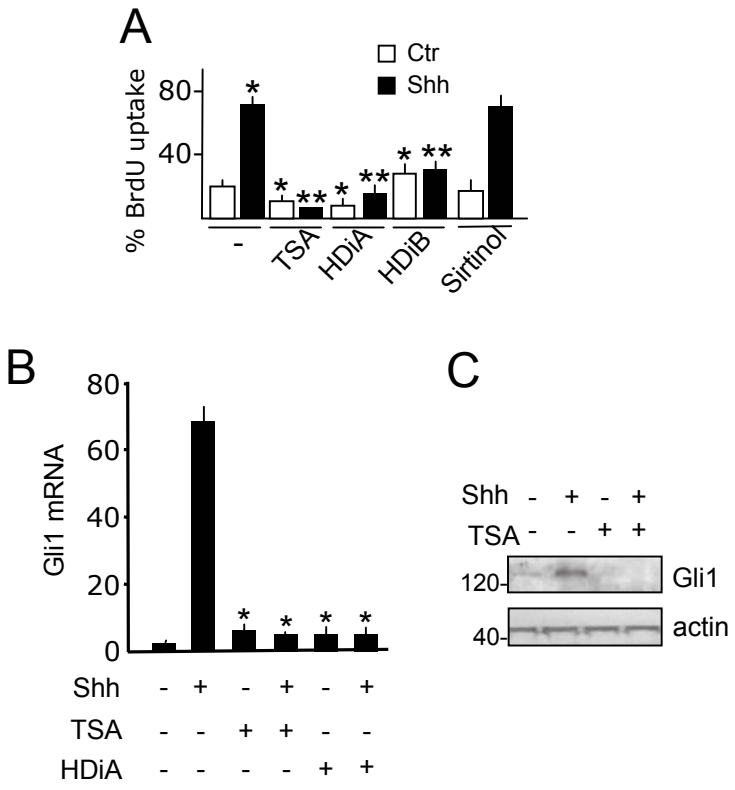

Figure S3 (**A**) Inhibition of HDAC1-3 abrogates Shh-induced proliferation of cerebellar GCPs. Primary GCPs isolated from 4-day old mice were cultured in the absence or in the presence of 3 microg/ml Shh for 48h and/or 1 microM TSA, or 2 microM HDiA or HDiB or 25 microM sirtinol in the last 24h and labeled for 18h with BrdU. Percentage of BrdU incorporating cells is indicated. * Shh or TSA or HDiA or HDiB vs control $p<0.05$; ** Shh+TSA or Shh+HDiA or Shh+HDiB vs Shh $p<0.05$. (**B**) Effect of HDAC inhibition on the suppression of Gli1 mRNA in cultured GCPs. GCPs were treated for 48 hours with 3 μg/ml Shh-N and, for the last 24 hours, with 1 microM TSA or 2 microM HdiA or vehicle control (-). Gli1 mRNA levels were evaluated by Q-PCR. * $p<0.05$. (**C**) GCPs were treated for 48 hours with Shh-N and for the last 24 hours with 1 microM TSA. Gli1 and actin control protein levels were evaluated by Western blot. Results in panels a, b are shown as means ± s.d. (n=3).

A

REN BTB domain sequence

β1 β2 A1 A2

VTLNVGGTLYSTTLETLTRFPDSMLGAMFRAGT

β3 A3

PMPPNLNSQGGGHYFIDRDGKAFRHILNFLRLG

A4 A5

RLDLPRGYGETALLRAEADFYQIRPLLDALRELE

B

```
                 B1      B2    A1          A2                  B3          A3
REN        18 --VTLNVG-GTLYSTTLETLTRFPDSMLGAMFRAGTPMPPNLNSQGGGHYFIDR-DGKAFRHILNFLRLG-----------RLD
Kv4.2      42 -LIVLNVS-GTRFQTWQDTLERYPDTLLGSSERDFFYHPETQ------QYFFDR-DPDIFRHILNFYRTG-----------KLH
Skp1        2 PSIKLQSSDGEIFEVDVEIAKQ--SVTIKTMLEDLGM----o-----DPVPLPNVNAAILKKVIQWCTHHKDD-o-IPVWDQEF
ElonginC   17 MYVKLISSDGHEFIVKREHALT--SGTIKAMLSGP------o-----NEVNFREIPSHVLSKVCMYFTYKVRYTNSSTEIPEFP

                      A4    **            A5
REN        87 LPRGYGETALLRAEADFYQIRPLL--DALRELEASQGTPAPT--------------------------------
Kv4.2     106 YPR-HECISAYDEELAFFGLIPEIIGDCCYEEYKDRRRENAE--------------------------------
Skp1       93 LKVDQGTLFELILAANYLD------IKGLLDVTCKTVANMIKGKTPEEIRKTFNIKNDFTEEEEAQVRKENQWC
ElonginC   95 IAPE--IALELLMAANFLDC-----------------------------------------------------
```

C

```
Cul1     1     msstrsqn---------phglkqigldqiwddlragiqqvytrqsm    37
               ...|.|:.         |..:.:..::.|||.|:..||::..:.:.
Cul3     1 msnlskgtgsrkdtkmrirafpmtmdekyvnsiwdllknaiqeiqrknns    50

Cul1    38 aksrymelythvytyctsvhqsnqargagvppskskkgqtpggaqfvgle    87
           ..| :.|||.:.|......|                              |.:
Cul3    51 gls-feelyrnaytmvlhkh---------------------------gek    72

Cul1    88 lykrlkeflknyltnllkdgedl---mdesvlkfytqqwedyrfsskvln   134
           ||..|:|.:..:|.|.::  ||:   ::.:.|:...|.|.|::.:..::.
Cul3    73 lytglrevvtehlinkvr--edvlnslnnnflqtlnqawndhqtamvmir   120

Cul1   135 gicaylnrhwvrrecdegrkgiyeiyslalvtwrdclfr--plnkqvtna   182
           .|..|::|.:|:      :..:..:|:|.|:.:||.:.|  .:...:...
Cul3   121 dilmymdrvyvq------qnnvenvynlgliifrdqvvrygcirdhlrqt   164

Cul1   183 vlkliekerngetintrlisgvvqsyvelglneddafakgptltvykesf   232
           :|.:|.:||.||.::...|....|..:.|||.         ..:||:|.|
Cul3   165 lldmiarerkgevvdrgairnacqmlmilgle---------grsvyeedf   205
```

D

```
Skp1      GTLFELILAANYLDIKGLLDVTCKTVAN
KCTD11    GETALLRAEADFYQIRPLLDALRELEAS
```

Figure S4 (**A**) REN BTB domain sequence. (**B**) Sequence alignment of representative mammalian BTB domains. Kv4.2 (PDB code 1NN7), Skp1 (PDB code 1LDK) and ElonginC (PDB code 1LM8) BTB domains were aligned on the basis of their three-dimensional structure. Human REN BTB, whose 3D structure is unknown, was aligned to the BTB domain of Kv4.2 on the basis of their sequences. Protein regions which were disordered in Skp1 and ElonginC structures have been indicated by open circles. α-helical, 3_{10}-helical and β-strand regions are colored in red, magenta and green, respectively. The core elements of the BTB fold are also shown and labeled B1 to B3 for the three conserved β-strands and A1 to A5 for the five α-helices. The asterisks denote the residues that have been mutated in REN mFY.(**C**) Sequence alignment of Cul1 and Cul3. Residues of Cul1 involved in the complex interface are colored in red. Residues of the interface conserved in Cul3 sequence are shown in green. (**D**) Sequence alignments of REN-BTB and Skp1 regions involved at the interface in the complex with Cul3 and Cul1, respectively. Residues of REN that have been mutated are highlighted in cyan.

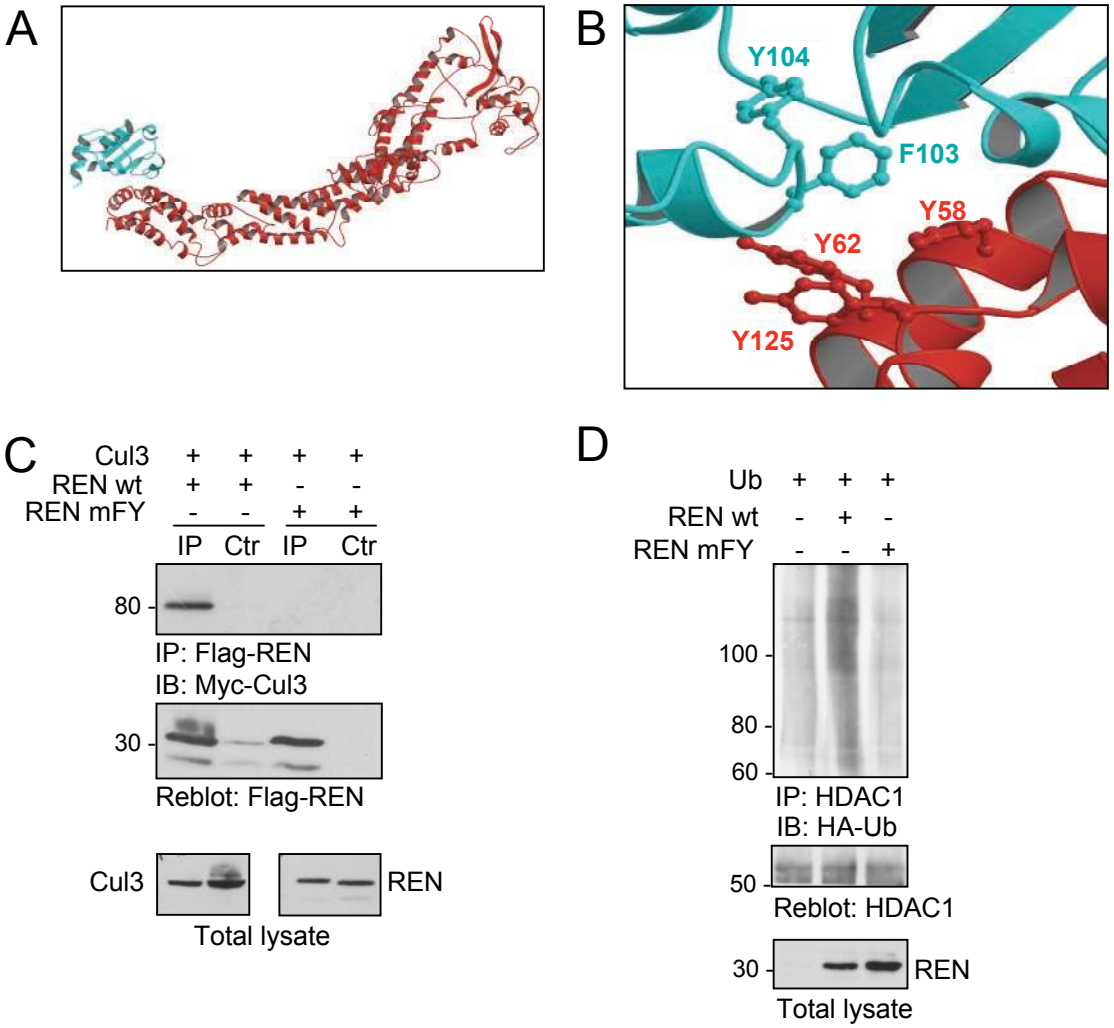

Figure S5 (**A**-**B**) Three-dimensional model of Cul3 (red)/REN-BTB domain (cyan) complex (**A**) and detailed view of the aromatic residues located at the interface (**B**) based on sequence homology with other BTB proteins and Cullins (Fig. S4). The model suggests that specific BTB or Cul3 aromatic residues may stabilize the interaction, as indicated by mutational studies shown in Fig. S5C,D and Fig. 6A. (**C**) Cul3 associates with REN, but not with its mutant REN mFY (F103K, Y104K). HEK293T cells were cotransfected with Myc-Cul3 or Flag-REN or Flag-RENmFY. IP was carried out with anti-Flag and immunocomplexes revealed with Myc antibody. The blot was reprobed with anti-Flag. Bottom panel, Cul3, REN and RENmFY levels in cell lysates. (**D**) REN, but not its mutant REN mFY, induce endogenous HDAC1 ubiquitination *in vivo*. Endogenous HDAC1 was immunoprecipitated from MG132 (50 microM)-treated HEK293T cells expressing the indicated proteins, followed by Western blot with HA antibody to detect conjugated HA-Ub. Blot was reprobed with anti-HDAC1. Bottom panel, REN and REN mFY protein levels in cell lysates.

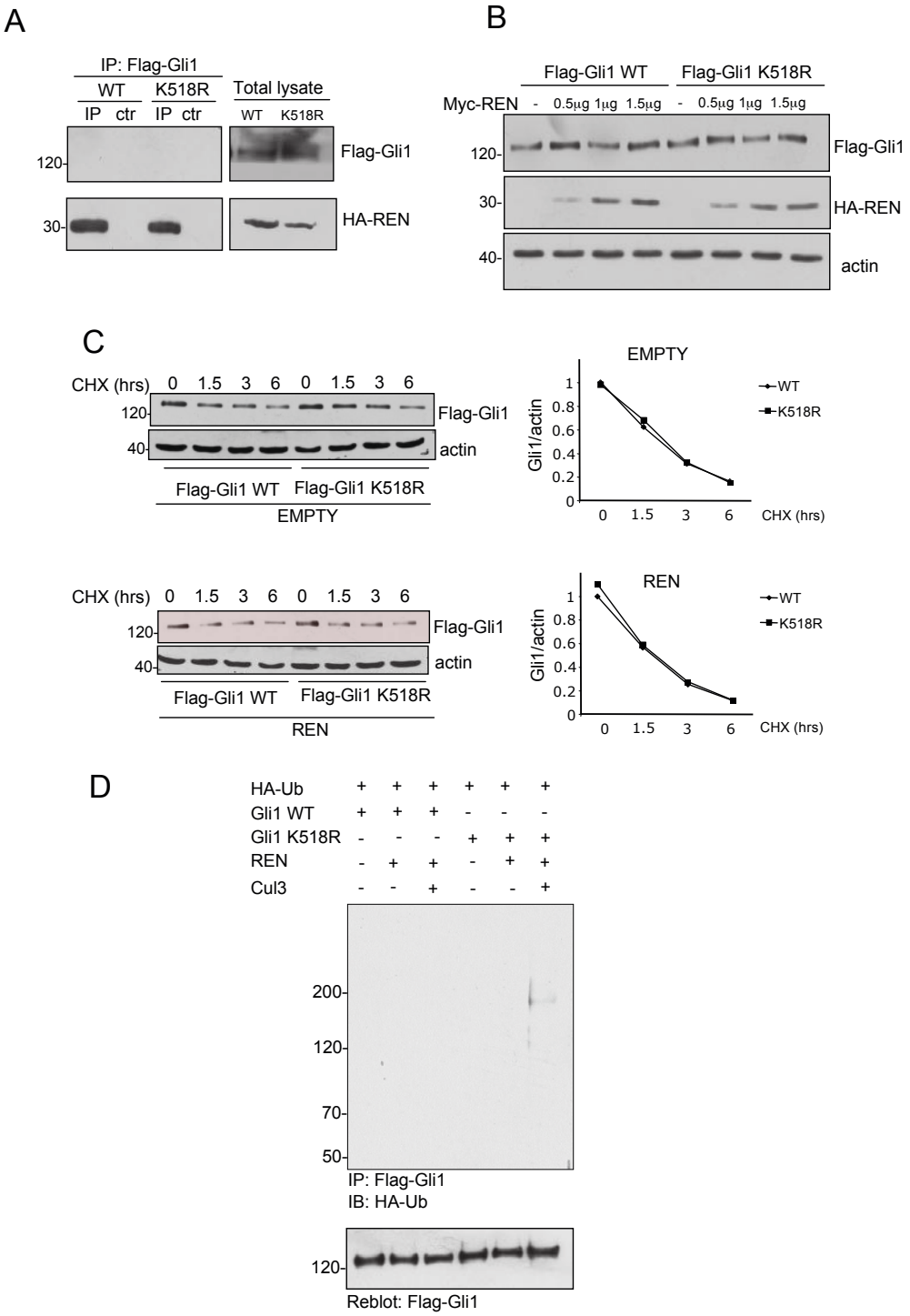

Figure S6 (**A**) Gli1 does not bind REN. HEK 293T cells were cotransfected with Flag-Gli1 WT or its K518R mutant and HA-REN and immunoprecipitated with anti-Flag agarose beads. Immunoblot was performed with the indicated antibodies. For negative controls (ctr) beads were pre-blocked with 0.1 mg/ml Flag peptide. Right (**B**) REN expression does not reduces the steady-state Gli1 protein levels. HEK293T cells were transfected with Flag-Gli1, in the presence or absence of increasing amounts of HA-REN and immunoblotted with the indicated antibodies. (**C**) Acetylation and REN does not affect Gli1 turnover. NIH 3T3 cells were transfected with Flag-Gli1 or its K518R mutant, in the presence or absence of HA-REN. After 24 hours, cells were treated with 30 microg/ml cycloheximide (CHX) for the indicated times. Immunobotting was performed with the specified antibodies. Right, densitometric analysis of Gli1/actin ratios shown in left panels. (**D**) REN does not promote ubiquitination of either Gli1 and its K518R mutant. Flag-Gli1 or its K518R mutant were immunoprecipitated from MG132 (50 microM)-treated HEK293T cells expressing the indicated proteins, followed by Western blot with HA antibody to detect conjugated HA-Ub. Immunoblotting was performed with the indicated antibodies.

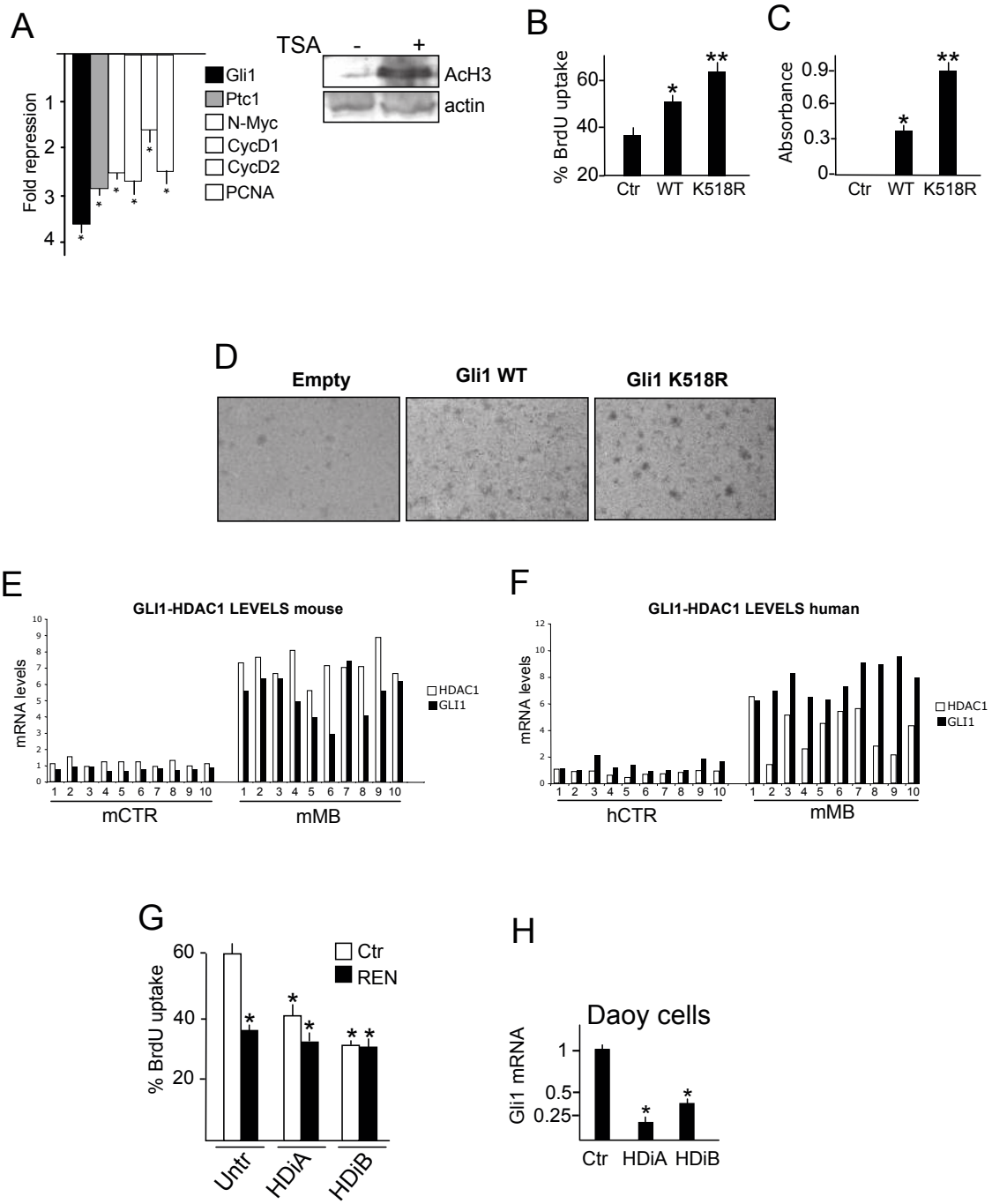

Figure S7 (**A**) Three day old mice (4 for each group) were injected subcutaneously with TSA (10 micrograms/g body weight) or DMSO. Six hours later, mice were sacrificed and the cerebellar GCPs isolated and pooled. Levels of mRNAs for the indicated targets were assessed by Q-PCR. The efficacy of TSA treatment in isolated GCPs was confirmed by Western blot analysis of acetylated histone H3 (right). Results are represented as fold repression and are calculated by dividing DMSO-treated by TSA-treated mRNA values for each gene. * p<0.01. (**B**-**C**) Effect of Gli1 K518R mutation on cell proliferation. D283 cells were transfected with empty (Ctr), Gli1 WT or Gli1 K518R vectors and BrdU (B) or MTS (C) assays were performed to evaluate cell proliferation. * WT vs control p<0.01; **K518R vs WT p<0.05. (**D**) Effect of Gli1 K518R mutation on cell transformation: representative picture. RK3E cells were transfected with the indicated vectors, grown for three weeks and stained with crystal violet. (**E**-**F**) Individual values of HDAC1 and Gli1 mRNAs (Q-PCR) in mouse primary Ptch1$^{+/-}$ MB (mMBs) (**B**) and in human primary MBs (hMBs) (**C**) versus normal cerebellum (ctr). (**G**) HDAC activity controls human MB cells proliferation and is required for REN-induced inhibition of growth. Daoy cells were transfected with REN or control vector for 48h and untreated or treated for the last 24h with HDiA or HDiB (left). *p < 0.05 versus untreated. (**H**) Inhibition of HDACs decreases Gli1 mRNA levels in MB cells. DAOY cells were treated with 2 microM HDiA or HDiB for 24 hours. Gli1 mRNA levels were evaluated by Q-PCR. *p<0.05. Results in panels a, b, c, g, h are shown as means ± s.d. (n=3).

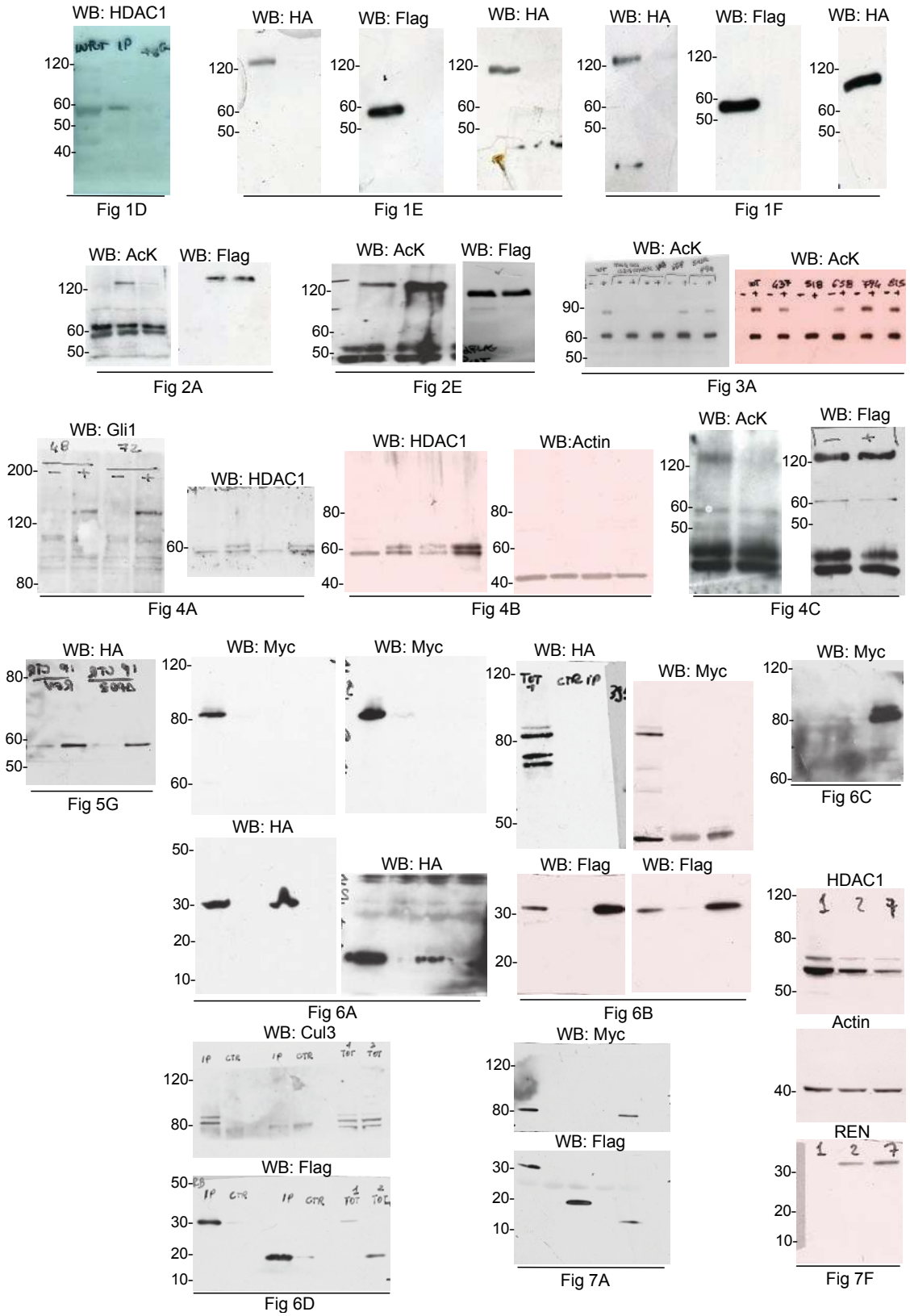

Figure S8 Full scan of key Western blots from indicated figures are shown.